chemosensors

MDPI

Review

Advances in Electrochemical Aptasensors for Targeted Detection in Biomedicine, Food Safety, and Environmental Monitoring

Wenting Shang [1,†], Peipei Zhou [1,†], Mengxue Liu [1], Guangxia Lv [1], Mengqi Sun [1], Yanxia Li [2,*] and Xiangying Meng [1,*]

[1] School of Medical Laboratory, Shandong Second Medical University, Weifang 261053, China; swt65582@stu.sdsmu.edu.cn (W.S.); zhoupp@sdsmu.edu.cn (P.Z.); liumx2004@stu.sdsmu.edu.cn (M.L.)
[2] College of Materials and Chemical Engineering, Minjiang University, Fuzhou 350108, China
* Correspondence: yxli09@163.com (Y.L.); mengxiangying85730@126.com (X.M.)
† These authors contributed equally to this work.

Abstract

Electrochemical biosensors have emerged as indispensable detection tools with rapid advancements in recent years, offering high sensitivity, specificity, and cost-effectiveness for quantifying diverse analytes, including amino acids, proteins, pathogens, cells, antigens, and organic/inorganic compounds, thereby advancing analytical detection technologies across multiple fields. Aptamers, synthetic in vitro-evolved ligands with exceptional binding affinity and stability, serve as superior biorecognition elements for electrochemical sensing interfaces. Compared with other bioreceptors such as antibodies, they are generally easier and faster to produce, more uniform between batches, and easier to modify chemically; they also maintain greater stability than protein antibodies or enzymes across varying pH, temperature, and ionic conditions, enabling targeted recognition and measurable signal transduction. This review systematically summarizes recent advances in electrochemical aptasensors across three core domains: biomedical diagnostics (covering tumor markers, infectious disease pathogens, cardiovascular and metabolic biomarkers), food safety monitoring (targeting antibiotics, mycotoxins, foodborne pathogens, and pesticide residues), and environmental hazard detection (including heavy metals, toxic compounds, and biotoxins). Key technological innovations such as nanomaterial modification, signal amplification strategies, and novel sensor architectures are highlighted. Additionally, it critically discusses prominent challenges, including complex matrix interference, limited aptamer repertoires, poor reproducibility, and lack of standardization, along with future prospects. This work aims to provide a comprehensive reference for the rational design, optimization, and clinical/field application of next-generation electrochemical aptasensing technologies.

Keywords: electrochemical aptasensor; biomedical detection; food safety monitoring; environmental hazard detection; aptamer recognition; nanomaterial modification

Check for updates

Received: 30 December 2025
Revised: 26 January 2026
Accepted: 6 February 2026
Published: 8 February 2026

Copyright: © 2026 by the authors. Licensee MDPI, Basel, Switzerland. This article is an open access article distributed under the terms and conditions of the Creative Commons Attribution (CC BY) license.

1. Introduction

Biosensors are analytical tools that identify target analytes in samples via biorecognition and signal transduction. Fundamentally, these devices are composed of three indispensable elements: a molecular recognition system, a signal transduction module, and a unit responsible for signal processing and output, integrating biochemical and transduction principles to enable qualitative, quantitative, or semi-quantitative analyte analysis [1,2].

Compared to traditional techniques, biosensors embed reagents within the system, avoiding the use of external reagents and extensive sample processing [3].

Among the diverse classes of biosensors (e.g., optical, electrochemical, acoustic, thermal), electrochemical sensors have drawn attention because they directly convert biochemical interactions into measurable electrical signals, simplifying signal transduction and reducing reliance on sophisticated equipment [4]. They allow rapid and sensitive detection with appropriate selectivity, operate simply at low cost, and show good compatibility with miniaturized or portable devices, making them potentially suitable for point-of-care and field applications [5,6]. Moreover, electrochemical sensing platforms can be readily integrated with microfabrication technologies and nanomaterial-based electrode modifications, which further support signal amplification and system miniaturization [7]. Compared with optical and other sensor types, they are generally less sensitive to environmental conditions, facilitating interface design and reliable signal readout [8,9]. These advantages make electrochemical sensors particularly suitable as platforms for aptamer-based biosensing, forming the core focus of this review.

The rapid development of electrochemical aptasensors is intrinsically linked to the distinctive characteristics of aptamers. Aptamers, short single-stranded sequences of DNA, RNA, and peptides, have become powerful biorecognition elements in biosensor design, replacing antibodies and other bioreceptor molecules. Nucleic acid aptamers in contemporary research usually have a molecular weight of 5 to 15 kDa (15 to 50 nucleotides), while peptide aptamers consist of 5 to 20 amino acid residues [10]. Oligonucleotide-based ligands are predominantly used in biosensor applications. As emerging materials, nucleic acid aptamers exhibit specific binding affinity toward diverse targets, such as proteins, peptides, amino acids, cells, metal ions, and drugs (Figure 1) [11]. In contrast to antibodies, aptamers are produced chemically, which generally makes them cheaper and quicker to obtain, more uniform between batches, and easier to modify in a controlled manner [12]. In addition, DNA aptamers maintain greater stability across different ionic strengths, pH values, temperatures, and storage conditions compared with protein antibodies and enzymes [13,14]. Therefore, aptamers represent a viable and promising option for use as biorecognition elements in electrochemical sensor development.

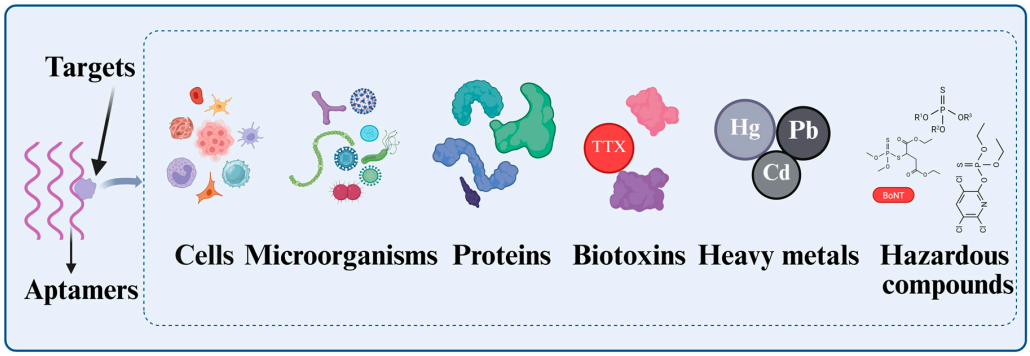


Figure 1. Types of assay targets for aptamer binding. The illustration was created by using BioRender (web version; https://biorender.com).

Aptamers for biosensors are typically obtained from a chemically synthesized combinatorial oligonucleotide library, which generally contains up to 10^{15} unique sequences. Each sequence consists of a central randomized region (20–50 nucleotides) flanked by two fixed primer regions used for PCR amplification [15]. These chemically synthesized oligonucleotides are then subjected to SELEX (Systematic Evolution of Ligands by Exponential Enrichment), an in vitro process that screens these libraries for sequences with high affinity to the target [16,17]. The four-step SELEX process (Figure 2) [18] involves incubating a

10^{15}-sequence combinatorial nucleic acid library exposed to the target, separating unbound sequences, eluting specifically bound ones, and amplifying them via PCR. Through iterative selection, high-affinity and specific aptamers are enriched and can be immobilized on sensing electrodes using strategies like covalent conjugation, biotin–avidin binding, or nucleic acid chain hybridization [19]. For example, DNA aptamers selected against glycated hemoglobin and thrombin have been successfully applied in electrochemical aptasensors, demonstrating high sensitivity and selectivity [20,21].

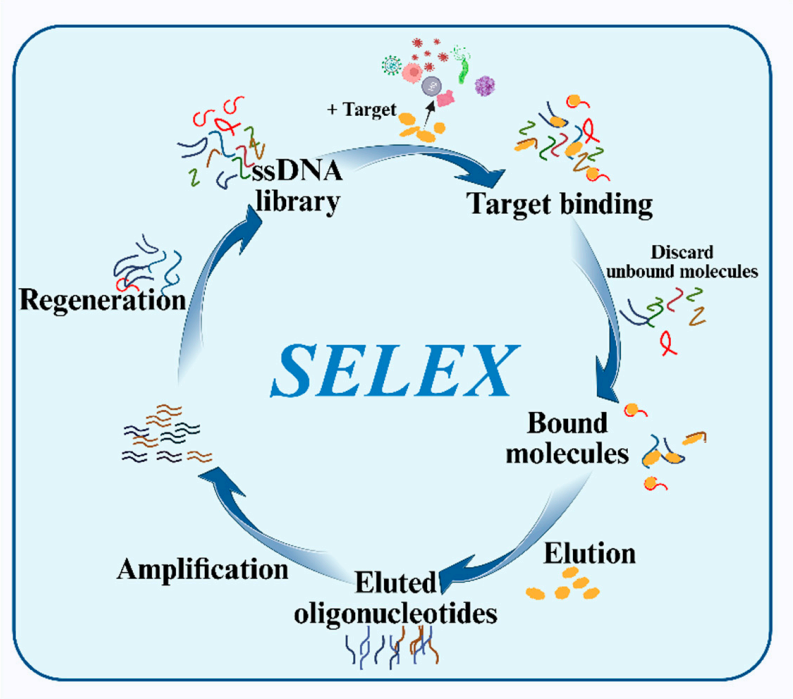


Figure 2. Schematic workflow of the SELEX process. The illustration was created by using BioRender (web version; https://biorender.com).

Leveraging the advantages of electrochemical techniques and aptamers, electrochemical aptasensors have attracted increasing research interest. Figure 3 schematically illustrates their working principle, which can be explained as follows: Aptamers, serving as biorecognition elements, specifically bind to target analytes (e.g., proteins, pathogens, DNA/RNA) in samples. When a target-containing sample enters the detection system, aptamers bind to the target. This binding induces changes in electrode-surface-modified nanomaterials and redox labels, generating an electrochemical signal. The sensor's detector captures these signals, and the transducer then converts and processes them. Finally, the processed signal is transformed into a format recognizable by receiving devices (e.g., computers, mobile phones, wearables), enabling qualitative or quantitative detection of the target analyte. Essentially, they leverage biorecognition and electrochemical transduction to transduce biomolecular interactions into electrical signals for target identification in samples. With ongoing progress in aptamer selection strategies and a growing grasp of electrochemical detection mechanisms, electrochemical aptamer-based sensors have achieved significant advancements in diverse application domains, including the identification of endogenous biomarkers closely linked to human health, identification of microbial targets (e.g., bacteria and viruses), monitoring of food safety parameters, and surveillance of environmental pollutants. Given the technological advantages enabled by the synergistic integration of nucleic acid aptamers and electrochemical detection, these biosensors are poised to become premier analytical tools in bioanalytical applications [22]. Most existing reviews primarily focus on specific analytes (e.g., antibiotics, heavy metals) or individual application fields

(e.g., clinical diagnostics, food safety). However, this review offers an integrated perspective, covering advancements and challenges across the three fields of biomedical, food safety, and environmental monitoring. This review aims to systematically summarize the latest developments in electrochemical aptasensor technologies within these key areas, with a particular emphasis on common design principles, signal amplification strategies, anti-interference mechanisms, and potential future challenges and development trends.

Relevant literature on electrochemical aptasensors was systematically retrieved from the PubMed and Web of Science databases using keywords such as "electrochemical aptasensor," "aptamer," and "biosensor." Studies were selected based on relevance, quality, and representativeness in medical diagnostics, food safety, and environmental monitoring, providing a solid foundation for this review to summarize recent advances and future trends in the field.

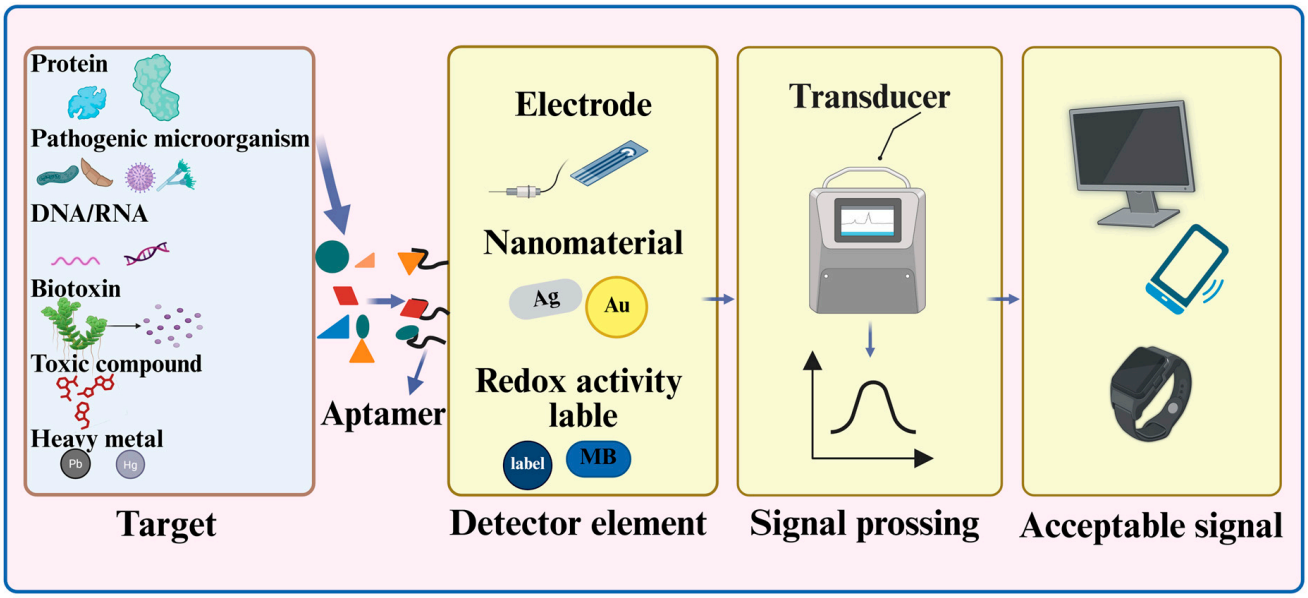


Figure 3. A brief working principle of electrochemical aptasensor. The illustration was created by using BioRender (web version; https://biorender.com).

2. Electrochemical Signal Transduction and Interpretation in Aptasensors

2.1. Interfacial Signal Modulation Upon Target Binding

Electrochemical measurements are carried out in a basic electrochemical system composed of an electrode—which serves as the physical interface for electron transfer and signal transduction—and an electrolyte, which provides ionic conductivity to complete the electrochemical circuit [23].

In typical aptasensing architectures, aptamers are immobilized at the electrode surface and act as dynamic molecular gates that regulate electron transfer between the redox probe and the electrode [24]. Most systems employ a redox-active reporter such as Methylene Blue (MB), whose electrochemical behavior is highly sensitive to interfacial physicochemical changes. Upon target binding, steric hindrance, electrostatic repulsion, and conformational rearrangements alter interfacial charge distribution and mass-transport pathways, thereby modulating electron-transfer kinetics and producing reproducible signal variations [25,26].

2.2. Key Electrochemical Readout Techniques and Analytical Parameters

Aptamer–target binding changes the electrode interface, and these alterations are converted into measurable electrical signals using several core electrochemical techniques, each with its own principle and type of readout.

Cyclic voltammetry (CV) is often the initial step to evaluate a sensor. By linearly sweeping the electrode potential back and forth, CV provides qualitative insight into electrode modifications, redox reversibility, and intermediates, helping to assess the electrode's behavior before quantitative measurements [27].

For quantitative detection, differential pulse voltammetry (DPV) and square wave voltammetry (SWV) are frequently used. These methods apply a series of potential pulses to minimize background currents, making the sensor highly sensitive to small changes. The peak current in the resulting voltammogram directly reflects the target concentration. They can also detect multiple analytes simultaneously if their redox potentials are sufficiently separated [28].

Electrochemical impedance spectroscopy (EIS) measures the electrode interface's resistance to electron flow over a range of frequencies. The key parameter, charge transfer resistance (Rct), rises when aptamer–target complexes form a barrier. EIS provides detailed insight into interfacial changes, can resolve simultaneous reactions, detect diffusion-limited processes, and often allows label-free detection [29].

Other approaches include amperometric techniques—such as constant potential amperometry or chronoamperometry (*i*–*t*, CA)—which monitor current over time for rapid, quantitative detection, and potentiometry, which records potential changes with minimal disturbance to the system, offering selective and label-free sensing. Together, these techniques provide the essential toolkit for electrochemical aptasensing, enabling sensitive and reliable target detection while clarifying key parameters such as Rct [30].

3. Advances in Electrochemical Aptasensors for Medical Detection

3.1. Electrochemical Aptasensors for Tumor Marker Detection

The global incidence of malignant tumors continues to rise, with the International Agency for Research on Cancer projecting that the number of new cancer cases will reach 30.2 million by 2040, accompanied by a corresponding increase in cancer-related mortality, a burden that is primarily associated with several major and commonly diagnosed cancer types, including lung, breast, colorectal, liver, and prostate cancers [31]. In clinical diagnostics, tumor biomarker detection has emerged as a preferred approach over traditional methods such as tissue biopsy, tumor imaging, and proteomics owing to its low invasiveness and cost-effectiveness [32]. Tumor markers, defined as substances produced by cancer cells or characteristically expressed in cancerous tissues, can be identified in patient tissues, body fluids, or excretions. These biomarkers are essential for identifying malignant tumors, assessing treatment efficacy, facilitating early diagnosis of tumor development and progression, and predicting tumor response to therapy [33]. Improving the efficiency of tumor biomarker detection is critical for advancing cancer research. Current assays, including enzyme-linked immunosorbent assay, fluorescence-based assays, and radioimmunoassay, are inherently limited by their requirement for skilled personnel, complex operational procedures, low sensitivity, slow analysis speed, and dependence on expensive high-end instruments [34]. Therefore, the development of fast and simplified detection strategies is urgently needed. Electrochemical biosensors employing aptamers have emerged as a significant research frontier for tumor biomarker detection [35]. This section elaborates on the recent progress in electrochemical aptasensor technologies for cancer biomarker detection.

Human Ecto-NOX disulfide-thiol exchanger 2 (ENOX2), a tumor-associated NADH oxidase critical for cancer cell proliferation and maturation, is prevalent across multiple malignancies. As an ecto-protein predominantly localized in cancerous cells, tissues, and biological fluids, ENOX2 represents a potential molecular biomarker for malignant tumor detection [36–38]. Building on this, Quansah et al. [39] designed an electrochemical biosensor for the efficient measurement of human ENOX2. In their work, the aptamer candidate

sequences were obtained by bead-based selection of biotinylated recombinant ENOX2 immobilized on avidin-coated magnetic beads, yielding specific oligonucleotides that were subsequently chemically synthesized for experimental validation. These synthesized oligonucleotides were then further engineered using computational modeling to adopt a two-state conformational system: a "bound state" enabling specific ENOX2 recognition and an "unbound state" with disrupted binding affinity. Upon ENOX2 binding, the aptamer undergoes a conformational change that reduces the redox current signal of MB, monitored by SWV. The biosensor demonstrated sensitive and specific ENOX2 detection with a limit of detection (LOD) of 1 nM (63 ng/mL), indicating its potential applicability in early cancer screening, where timely ENOX2 detection could support preclinical intervention. However, the sensor still exhibits certain limitations, including noticeable signal variability and the lack of systematic validation in complex real clinical samples. Moreover, as this strategy relies on a single biomarker, its diagnostic specificity in heterogeneous clinical matrices may be inherently limited. These factors may affect the robustness and clinical translatability of the proposed platform.

Among liquid biopsy-derived human biomarkers, circulating tumor cells are regarded as the most reliable and specific indicators for early clinical cancer diagnosis [40,41]. Shed from primary tumors into peripheral blood, circulating tumor cells are intimately linked to tumor metastasis and recurrence. However, their detection remains challenging due to their extremely low abundance (typically <10 cells/mL) and inherent fragility [42]. Currently, the main circulating tumor cells detection methods, including immunoaffinity-based assays and microfluidic-based platforms, are generally limited by complex manufacturing requirements, restricted blood sample volume, and typical sampling frequency. Moreover, most rely on single-biomarker detection, which restricts sensitivity and specificity. To address this, Peng et al. [43] constructed an electrochemical biosensor featuring a dual-recognition control mode. The sensor features two chemically synthesized aptamer hairpin probes targeting tumor-associated cell surface proteins mucin 1 and epithelial cell adhesion molecules (EpCAM), respectively. These probes are immobilized on a gold electrode surface modified with tetrahedral DNA nanostructures (TDNs), which provide precise spatial orientation for aptamer presentation. Binding of aptamer hairpins to mucin 1/EpCAM triggers a rolling circle amplification (RCA) reaction, generating amplified electrochemical signals. The sensor achieves an LOD of 3 cells/mL, outperforming single-recognition systems by requiring simultaneous binding to both biomarkers, thus reducing false positives. This dual-recognition mode demonstrates high stability and anti-interference capability in whole blood samples, holding promise for clinical cancer diagnostics and therapeutic monitoring. Nevertheless, although the dual-recognition strategy and RCA-based signal amplification significantly improve sensitivity and selectivity, the sensor relies on multiple sequential hybridization and amplification steps, which inevitably increase operational complexity and time consumption. Moreover, the requirement for carefully prepared DNA nanostructures and precise probe assembly may limit large-scale fabrication and routine clinical translation.

Exosomes themselves hold significant promise for cancer theranostics, prompting Liu et al. [44] to develop a split aptamer-mediated regenerative temperature-sensitive (SMRT) electrochemical biosensor. The sensor employs a split aptamer system comprising two fragments: both split-a and split-b were chemically synthesized, split-a was immobilized on a pretreated gold electrode via thiol-Au covalent bonding after tris(2-carboxyethyl)phosphine reduction, while split-b was conjugated with MB. In the presence of exosomes, split-a and split-b form a sandwich structure on the electrode surface, enabling specific capture and voltammetric detection. The electrodes were part of a three-electrode system comprising a gold working electrode (3 mm diameter), a saturated calomel reference electrode, and a Pt

auxiliary electrode. Rinsing the electrode with phosphate-buffered saline (PBS) at 37 °C disrupts the aptamer-exosome complex, regenerating the sensor within 30 s for repeated use. The SMRT biosensor exhibits an LOD of 1.5×10^6 particles/mL, characterized by high responsiveness and rapid regenerability. Signal intensity, currently limited by inherent aptamer-electrode interactions, may be further enhanced via enzyme integration or other amplification strategies. Notably, this represents the first renewable electrochemical biosensor utilizing split aptamers for tumor exosome detection, offering a cost-effective and innovative paradigm for regenerative biosensing technologies. However, as acknowledged by the authors, the main limitation of the SMRT biosensor is its relatively low current output. Although the LOD is comparable to most reported methods, the low signal mainly restricts further signal amplification rather than the current detection capability. The authors therefore suggest that enzyme- or DNA nanotechnology-based amplification strategies may be explored to enhance the signal. In addition, while the temperature-controlled regeneration strategy is presented as a gentle and simple advantage, its performance under broader clinical temperature variations and long-term operating conditions has not yet been systematically evaluated. Further validation in more complex biological environments is therefore warranted to confirm the robustness of this platform.

Breast cancer constitutes a major public health concern for women worldwide. Circulating exosomes released by cancer cells (including circulating tumor cells) carry membrane proteins reflecting tumor physiology [45], and these membrane proteins are expected to function as biomarkers for breast cancer detection, treatment monitoring, and outcome evaluation [46,47]. Cheng et al. [48] capitalized on this by engineering a bimodal aptasensor that integrates colorimetric and electrochemical detection for simultaneous analysis of exosomal Programmed death ligand 1 (PD-L1) and mucin 1, involving hybridization of exosome-specific aptamers to DNA probes with a 3:1 split G-quadruplex motif that folds into a heme/G-quadruplex DNAzyme upon target binding, generating both colorimetric signals, allowing rapid visual readout suitable for simple or on-site detection, and electrochemical signals, measured using a conventional three-electrode system comprising a gold working electrode, a Pt auxiliary electrode, and an Ag/AgCl reference electrode by DPV, enabling precise quantitative measurement with high sensitivity and extended linear range. This dual-mode design offers improved detection performance over unimodal sensors, reducing false positives and combining simplicity with cost-effectiveness, making it a promising tool for non-invasive breast cancer diagnostics.

Among key diagnostic biomarkers for breast cancer, Human Epidermal Growth Factor Receptor 2 (HER2), an amplified oncogene encoding a transmembrane tyrosine kinase linked to ~20% of breast cancers, is crucial for tumor progression [49,50]. Ferreira et al. [51] designed and refined an electrochemical aptasensor for detecting the HER2 protein, comparing two gold screen-printed electrode (AuSPE) platforms: a binary self-assembled monolayer (SAM) composed of HER2-specific thio-DNA aptamer and 1-mercapto-6-hexanol (MCH), and a ternary SAM incorporating the same aptamer, MCH, and 1,6-hexanedithiol (HDT). In undiluted human serum (HS), the binary SAM achieved a detection limit of 179 pg/mL with a sensitivity of 4.32% per decade, while the ternary SAM, benefiting from HDT's antifouling properties to reduce non-specific adsorption, showed a slightly lower detection limit of 172 pg/mL and a sensitivity of 4.12% per decade, highlighting the improved biosensing performance of the ternary architecture. While the ternary SAM shows reduced nonspecific adsorption, the overall improvement over the binary SAM is relatively limited, as reflected by the very similar detection limits in undiluted serum (179 pg/mL vs. 172 pg/mL). The authors also report that serum proteins, such as albumin, can interfere with aptamer–HER2 binding, leading to decreased sensitivity. Therefore,

further evaluation in more complex clinical samples would be valuable to confirm the robustness of this sensing strategy.

Prostate cancer (PCa) is a leading malignancy and cause of cancer-related mortality in men, garnering global attention for its clinical urgency [52]. Early diagnosis remains pivotal for therapeutic success, with biomarkers like prostate-specific antigen (PSA) serving as critical diagnostic targets. Recent advancements highlight the utility of dual-biomarker detection in enhancing diagnostic efficiency, as demonstrated by an electrochemical sensor capable of simultaneous quantification of PSA and sarcosine [53]. The sensor employs a hierarchical flower-like molybdenum disulphide (MoS_2) nanostructure as a functional interface, engineered to enhance DNA hybridization efficiency. Complementing this, spherical SiO_2 nanoprobes are functionalized with electroactive labels and DNA probes, enabling electrochemical signal amplification. This design achieves low LODs of 2.5 fg/mL for PSA and 14.4 fg/mL for sarcosine. Notably, the sensor demonstrates the potential for accurate, one-step screening of cancer patient serum samples for early PCa detection, leveraging simultaneous measurement of PSA and sarcosine. It should be noted that, the fabrication of the MoS_2 interface and the signal-amplifying SiO_2 nanoprobes involves multiple preparation steps, which may affect reproducibility and large-scale implementation. Therefore, further optimization and validation would be needed before clinical translation.

As noted, the translation of electrochemical aptasensors for cancer diagnostics is often limited by complex fabrication, multi-step signal amplification, and insufficient clinical validation, yet their outstanding analytical performance makes them highly promising. As summarized in Table 1, the breadth and diversity of reported studies provide a solid foundation for advancing clinically applicable systems.

3.2. Electrochemical Aptasensors for the Detection of Other Diseases

Beyond malignant tumors, many diseases in the human body produce or have unique biomarkers that exist in body fluids or tissues, usually in the form of nucleic acids, proteins, pathogen-specific antigens/antibodies, and some metabolites. Identifying these biomarkers is crucial for the timely diagnosis and management of diseases.

Table 1. Representative applications of electrochemical aptasensors for cancer biomarker detection.

Analyte	Key Electrode Material	Disease Type	Electrochemical Methods	Electrochemical Conditions (Electrolyte Solution; Reference Electrode)	LOD	Detection Range	Reference
mucin 1	MXene−Au	Breast cancer	CV/DPV	PBS (0.1 M, pH 7.4) + 1 M KCl; Ag/AgCl	0.65 fg/mL	1 fg/mL–10 ng/mL	[54]
Carcinoembryonic antigen(CEA)	High-entropy alloy nanoparticles/Fe-metal–organic frameworks/Glassy carbon electrode (GCE)	Various cancers	DPV	5 mM $[Fe(CN)_6]^{3-/4-}$ + 0.1 M KCl; Ag/AgCl	0.115 fg/mL	10 μg/mL–1 fg/mL	[55]
CEA	NH_2-Vertically ordered mesoporous silica films/Polarized screen-printed carbon electrode (p-SPCE)	Various cancers	DPV	0.1 M KCl + 1.25 mM $[Fe(CN)_6]^{3-/4-}$; Ag/AgCl	24 fg/mL	100 fg/mL–100 ng/mL	[56]
PSA	Manganese oxide/Pencil graphite electrode	PCa	ESI	PBS (0.1 M, pH 7.4) + 5 mM $[Fe(CN)_6]^{3-/4-}$ + 0.1 M KCl; Ag/AgCl	0.009–0.035 nM (pH < pI, isoelectric point)	0.009–0.035 nM (pH < pI, isoelectric point)	[57]
CEA	Zirconia-gold nanoparticles (ZrO_2-AuNPs)	Lung cancer	DPV	5 mM $[Fe(CN)_6]^{3-/4-}$ + 0.10 M KCl; Ag/AgCl	42.504 fg/mL	0.01–10^4 pg/mL	[58]
HER2	Zinc oxide tetrapods-Potassium perylene tetracarboxylate	Breast cancer	SWV	PBS (0.1 M, pH 7) + 100 μM MB; Ag/AgCl	0.58 fg/mL	1 fg/mL–10 μg/mL	[59]
exosomes	CD63 aptamer/Gold electrode	Breast cancer	Amperometric (*i*–*t*)	0.4 mM TMB + 10 mM H_2O_2; -	1×10^2–1×10^7 particles/mL	45 particles/mL	[60]
PD-L1	DNA nanotetrahedron/Gold electrode	Breast cancer	DPV	PBS (0.1 M, pH 7.0) + 2 mM H_2O_2 + 3 mM HQ; -	7.76 pg/mL	0.01–1000 ng/mL	[61]
exosomes	Gold electrode/SYL3C aptamer	Non-small-cell lung cancer	DPV	20 mM Tris-HCl (pH 8.0) + 20 mM NaCl; Ag/AgCl	234 particles/mL	3.45×10^2 to 3.45×10^7 particles/mL	[62]
Sarcosine	$CuCo_2O_4$ nanosheets	PCa	EIS	5 mM $[Fe(CN)_6]^{3-/4-}$ + 0.10 M KCl; Ag/AgCl	350 fM	1 pM to 8 μM	[63]
Carbohydrate antigen 19-9	Highly porous carbons/Polyethylenimine (PEI)-AuNPs	Gastric/Pancreatic cancers	DPV	0.20 M acetate buffer (pH 4.5); Ag/AgCl	0.039 U/mL	0.10–200 U/mL	[64]
Vascular endothelial growth factor	Carbon dots	Lymphoma	DPV	PBS (0.1 M, pH 7.4); Ag/AgCl	0.112 pg/mL	0.34–34×10^6 pg/mL	[65]
Alpha-fetoprotein (AFP)	Polydimethylsiloxane/Au	Hepatocellular carcinoma (HCC)	DPV	PBS (pH 7.5) + 20 mM HQ + 30 mM H_2O_2; Ag/AgCl	0.71 pg/mL	0.01–300 ng/mL	[66]
AFP	MoS_2/Fe_3O_4	HCC	DPV	PBS (0.1 M, pH 7.4); -	0.3 pg/mL	0.001–0.1 ng/mL and 0.1–100 ng/mL	[67]
AFP	Fe_3O_4/α-Fe_2O_3/Au	HCC	DPV	-	1.31 pg/mL	10 pg/mL–1 μg/mL	[68]

3.2.1. Detection of Infectious Diseases

Pathogens (e.g., bacteria, viruses, fungi) and their secreted toxins can serve as crucial diagnostic biomarkers in infectious diseases, and their identification is essential to support early diagnosis. Among the various detection strategies, electrochemical aptasensors have emerged as promising tools for infectious disease detection by enabling sensitive electrical readout of interactions with pathogen-derived biomarkers. In these systems, aptamers specifically recognize pathogen-associated targets, such as surface antigens or secreted proteins. The binding of these targets induces interfacial changes at the electrode, which are transduced into measurable variations in current, voltage, or impedance, thereby enabling sensitive and selective pathogen detection [69].

Among these, tuberculosis (TB), resulting from infection with *Mycobacterium tuberculosis* (MTB), represents significant public health challenges [70]. Conventional MTB detection methods, such as acid-fast staining, tuberculin testing, bacterial culture, and PCR, suffer from time-intensive procedures and low throughput [71,72], driving the urgent need for efficient diagnostic technologies. Huang et al. [73] designed an electrochemical aptasensor with a dual-signal output approach for early secreted antigenic target 6 (ESAT-6) detection. The sensor utilized a novel MXene/fullerene nanoparticle (C_{60}NP)/Au@Pt nanocomposite that integrated the electrochemical redox activity of C_{60}NPs and the electrocatalytic activity of Au@Pt nanoparticles for signal generation and amplification. An ESAT-6-specific aptamer was conjugated to Au@Pt to serve as the signaling element, while MoS2-loaded AuNPs acted as the sensing interface; the dual signal outputs arose from the synergistic effects of the redox activity of C_{60}NPs and the electrocatalytic activity of Au@Pt. The sensor achieved LODs of 2.88 fg/mL (via DPV) and 13.50 fg/mL (via amperometric *i*–*t* curve, IT) within linear ranges from 100 fg/mL to 50 ng/mL. By comparison, conventional MTB detection methods generally exhibit relatively high practical detection thresholds. For example, sputum smear microscopy typically requires 5000–10,000 CFU/mL for reliable detection [74], while routine real-time PCR assays, including multiplex PCR approaches used for smear-negative clinical samples, typically report LODs around 10^3 copies/mL. Although advanced molecular techniques, such as nested PCR or digital PCR, can achieve single-copy-level sensitivity, they typically require sophisticated instruments, involve multiple procedural steps, and entail longer assay times and higher costs, which limit their suitability for resource-limited or point-of-care settings [75]. In this context, aptamer-based electrochemical sensors, which achieve femtogram-level detection, offer a compelling alternative by enabling substantially lower practical LODs. They also combine high specificity provided by aptamers for pathogen-associated targets with rapid signal readout enabled by electrochemical transduction, and are compatible with miniaturized or point-of-care platforms. Nevertheless, the practical translation of this high-performance sensor could be constrained by its complex nanomaterial fabrication process and the relatively limited clinical validation performed on a selective serum sample set.

Studies have shown that in recent years, the incidence of digestive diseases caused by *Helicobacter pylori* (*H. pylori*) infection has been escalating, causing physical and psychological burdens on patients and increasing the risk of cancer. *H. pylori* is strongly associated with gastritis, gastroduodenal ulcer, and gastric cancer [76–78], making its detection crucial for digestive disease management. Roushani et al. [79] developed a gold nanostructure-supported hollow nitrogen-doped carbon nanocapsule (Au@HNC) platform. The Au@HNC nanocomposites feature a high density of catalytic sites and an extensive surface area, enabling efficient immobilization of specific nucleic acid aptamers for highly selective *H. pylori* detection. The aptasensor demonstrated a linear response within the range of 1×10^2 to 1×10^7 CFU/mL and an LOD of 33 CFU/mL, reflecting its potential for high sensitivity relative to conventional methods, such as histopathology and culture,

whose performance can be affected by factors such as bacterial load [80]. By combining aptamer specificity with rapid, quantitative electrochemical readout, this platform offers a promising strategy for sensitive and potentially point-of-care H. pylori detection. Nevertheless, while the aptasensor demonstrates excellent sensitivity and selectivity, its clinical validation is still limited, as it was tested only on spiked (diluted) serum samples. Furthermore, despite being eco-friendly, the fabrication process involves multiple steps, which could affect the scalability of this technology.

Building upon recent progress in infectious disease detection, electrochemical aptasensor development holds promise for precise etiological evidence supporting early infection diagnosis in clinical practice and securing a critical therapeutic window for the implementation of targeted anti-infective therapies.

3.2.2. Detection of Cardiovascular Diseases

Common cardiovascular diseases (CVDs), including coronary artery disease, myocardial infarction, and heart failure, often lead to multi-organ failure and fatal outcomes. Among them, acute myocardial infarction (AMI) stands out as a major lethal CVD globally, and cardiac troponin I (cTnI) serves as the primary biomarker in clinical diagnosis [81]. Chen et al. [82] designed a sensitive electrochemical sensor based on a sandwich configuration for cTnI detection, as shown in Figure 4. The sensor features Au-loaded zirconium-carbon (Au/Zr-C) electrodes prepared via carbonization-reduction, exhibiting large effective area, porous structure, and superior conductivity. Snowflake-like PtCuNi catalysts with excellent catalytic stability were synthesized as labeling materials, conjugated to aptamer 2. Through sequential incubation of aptamer 1, cTnI, and aptamer 2-PtCuNi on Au/Zr-C modified electrodes, the sensor exhibited a linear response between 0.01 pg/mL and 100 ng/mL, with a LOD as low as 1.24×10^{-3} pg/mL. Moreover, even at concentrations 100-fold higher than that of cTnI, the signal responses of mixed samples containing cTnI and interfering proteins (e.g., bovine serum albumin, casein, human serum albumin, and human serum immunoglobulin G) were comparable to that of cTnI alone, indicating good anti-interference capability and high selectivity, supporting its potential for clinical AMI diagnostics. In addition to cTnI, myoglobin serves as an early diagnostic biomarker for AMI due to its rapid release from damaged cells and early blood concentration elevation. Zhu et al. [83] reported an aptamer sensor comprising a carbon nanotube (CNT)-AuNP-glucose oxidase bioanode and a CNT-AuNP-aptamer biocathode. In the absence of myoglobin, glucose oxidation by glucose oxidase at the bioanode generates electrons that reduce $[Fe(CN)_6]^{3-}$ to $[Fe(CN)_6]^{4-}$ at the biocathode, yielding high open-circuit voltage (EOCV). Upon myoglobin binding to the biocathode aptamer, the redox probe's electron transfer is inhibited, causing EOCV decline. A broad linear range between 0.1 and 1×10^4 ng/mL was achieved for the sensor, with an LOD of 0.011 ng/mL, potentially enabling early AMI detection. However, it is important to note that, although the self-powered aptasensor demonstrates high sensitivity (LOD = 0.011 ng/mL) and good selectivity in complex samples, further clinical testing is necessary to confirm its reliability. While the sensor performs well under lab conditions, real-world scenarios, including potential interference from other biomolecules, require additional validation. Furthermore, the stability of the aptamer immobilization (via Au−S bonds) needs to be tested under varying pH and temperature conditions to ensure long-term durability in clinical applications.

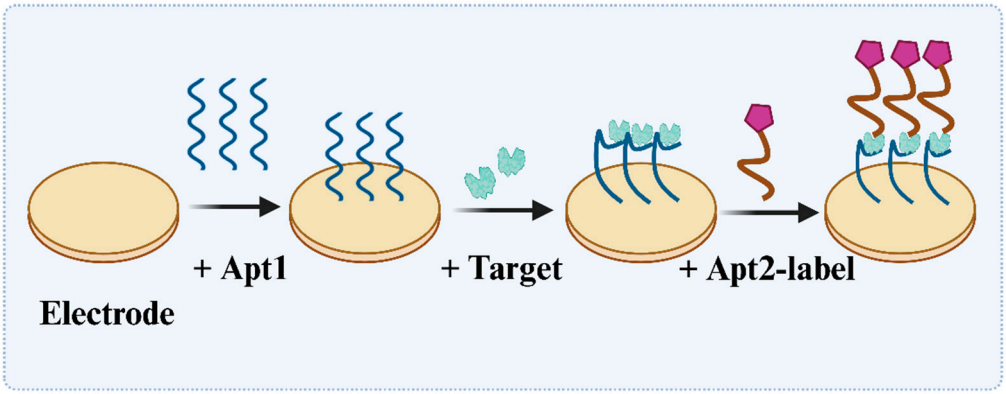


Figure 4. Schematic mechanism of sandwich-type aptamer sensors. Apt2-label: Apt2 combined with a detection element for biosensing, used for target capture and signal enhancement in a sandwich-type assay. The illustration was created by using BioRender (web version; https://biorender.com).

3.2.3. Detection of Inflammatory and Metabolic Diseases

Inflammatory and metabolic disorders are two major disease categories, and the detection of their biomarkers is crucial for clinical management and prognosis. Inflammatory diseases are often associated with dysregulated immune responses, where cytokines such as interleukins and interferon-γ (IFN-γ) serve as key indicators of immune activity and inflammatory signaling; imbalances in cytokine levels can lead to systemic pathological changes. Metabolic disorders involve disruptions of physiological homeostasis, with hormones such as cortisol and thyroxine playing critical roles in regulating carbohydrate, lipid, and protein metabolism; abnormalities in hormone levels can directly affect metabolic balance [84–86]. Both cytokines and hormones provide important information for disease diagnosis and monitoring. However, current clinical detection techniques often suffer from limited sensitivity and operational convenience, highlighting the urgent need for advanced biosensing platforms that combine high sensitivity, specificity, and practical applicability.

Cytokines, as bioactive molecules, function as crucial biomarkers for monitoring and predicting disease progression in inflammation-associated disorders [87]. Notably, these molecules, including the important marker interleukin-6 (IL-6), are present in trace amounts in sweat [88]. To tackle this challenge, Chu et al. [89] designed a wearable electrochemical biosensor capable of real-time IL-6 monitoring in sweat. The sensor was fabricated by coupling redox probe-modified IL-6 aptamers onto the surface of CNT/graphene composite fibers to form a sensing fiber, which was then integrated with commercial textile materials. This innovative design enables the sensor to achieve a broad detection range from 1 pg/mL to 100 ng/mL and a low LOD of 280 fg/mL. Furthermore, by simply replacing the aptamers, the sensor can be adapted to detect other low-concentration biomarkers in sweat. Owing to its flexibility and breathability, the fabric-based system offers excellent wearability and can be applied to various body parts. Despite the need to overcome certain interfering factors in future practical applications, this wearable sensing platform represents a significant advancement, providing a novel perspective for personalized real-time health monitoring.

Cytokine storm, a systemic inflammatory response syndrome, is characterized by uncontrolled elevation of circulating cytokines. In 2020, David C. Fajgenbaum and Carl H. June defined it as a clinical entity marked by hypercytokinemia, systemic inflammation, and severe secondary organ damage, posing significant health risks [90]. Cytokine release syndrome progression is linked to dysregulation of pro-inflammatory/anti-inflammatory cytokine networks, with interleukin-10 (IL-10), IL-6, and IFN-γ consistently elevated in patient sera [91]. Noh et al. [92] developed a microfluidic chip integrating MXene (Ti_3C_2), a 2D nanomaterial with exceptional electrical conductivity and mechanical strength, paired with dual Au microgap electrodes and tumor necrosis factor-α (TNF-α)/IFN-γ aptamer

bioprobes for specific recognition. Alternating current electrothermal flow (ACEF) is applied to actively drive target molecules toward the sensor surface, accelerating aptamer-target binding and reducing diffusion-limited detection time. Biomarkers are quantified via EIS by measuring Rct changes. The sensor achieves buffer LODs of 0.15 pg/mL for TNF-α and 0.12 pg/mL for IFN-γ over a detection range of 1 pg/mL to 10 ng/mL within 10 min, and demonstrates serum compatibility with LODs of 0.25 pg/mL and 0.26 pg/mL in 10% HS. By combining ACEF with MXene-enhanced electrodes, the biosensor not only enables rapid detection but also maintains high selectivity and reproducibility. Despite the sensor's impressive potential, the authors themselves underscore two key limitations. First, further interference testing with other cytokines and biomolecules (e.g., interleukins, growth factors) is needed to confirm its specificity and avoid cross-reactivity. Second, real clinical validation across diverse patient populations is essential, as current promising serum compatibility results are based on artificial samples that may not reflect clinical complexities. These aspects require thorough investigation before the biosensor can be deemed reliable for widespread clinical use. Wang et al. [93] reported a graphene–nafion composite aptasensor for undiluted biofluids, which employs aptamer-modified films to suppress non-specific adsorption and generates drain-source current changes via aptamer-biomarker binding, enabling continuous monitoring of IFN-γ in sweat over a detection range of 0.015 to 250 nM and an LOD as low as 740 fM. This flexible, renewable platform, regenerable via simple rinsing, represents a breakthrough for real-time cytokine storm diagnostics.

Hormones are bioactive molecules that regulate key metabolic processes. Among them, glucocorticoids as crucial members of the hormone family require particular monitoring attention. Taking cortisol as an exemplary case, this pivotal glucocorticoid orchestrates critical physiological processes, including glucose/lipid/protein metabolism, anti-inflammatory responses, and growth regulation, with profound implications for psychological and physiological homeostasis [94,95]. Dysregulation of cortisol levels has been linked to numerous pathologies, underscoring the clinical urgency of sensitive detection methods. Karuppaiah et al. [96] pioneered an electrochemical biosensing platform by conjugating the redox reporter MB to a cortisol-specific aptamer. The aptamer was chemically modified with-NH_2 at the 5′-end and -SH at the 3′-end, enabling covalent attachment of MB and site-specific immobilization on a Au electrode surface. This strategy yielded the first electrochemical cortisol aptasensor featuring a detection range of 0.05 to 100 ng/mL, laying the foundation for endocrine-related diagnostic applications. Subsequently, Rahmati et al. [97] reported a label-free approach using metal–organic framework (MOF)-derived Ni-P nanorods as aptamer carriers, with fabrication involving hydrothermal synthesis of Ni-MOF precursors, followed by phosphorylation to generate Ni-P nanorods that enhanced aptamer loading via surface chemistry, and EIS for label-free detection in redox probe solutions. This sensor exhibited an ultra-broad linear range from 0.1 fM to 700 nM and an exceptionally low LOD of 10 aM, alongside superior reproducibility and stability, whereby the MOF-derived nanomaterial strategy offers a paradigm shift for ultrasensitive cortisol monitoring in clinical settings.

Thyroxine, a key thyroid hormone, plays a pivotal role in human physiology, with serum concentrations typically ranging from 8 to 18 pg/mL [98,99]. Secreted by the thyroid gland into the bloodstream, thyroxine rapidly binds to plasma proteins, regulating metabolic rate, oxygen utilization, and protein synthesis. Conventional detection methods, including chromatography and mass spectrometry, suffer from complexity and time-consuming procedures [100,101], driving the advancement of electrochemical aptamer sensors as viable alternatives. Park et al. [102] constructed an electrochemical biosensor featuring a DNA three-way junction bioprobe immobilized on porous rhodium nanoplate-modified gold electrodes. The three-way junction structure integrated target recognition

and signal reporting functions, while porous rhodium nanoplate enhanced electrode surface roughness to facilitate electrochemical signaling. Through CV and EIS analyses, the sensor exhibited detection limits of 10.33 pM in buffer and 11.41 pM in clinical samples, demonstrating potential for improved sensitivity and convenience compared with traditional methods. Similarly, Kashefi-Kheyrabadi et al. [99] reported a nano-hybrid platform combining $Ti_3C_2T_x$ MXene and MoS_2 nanosheets on carbon electrodes, which was subsequently electroplated with 3D gold nanostructures. The $Ti_3C_2T_x/MoS_2$ NS composite optimized electrode physicochemical properties and promoted gold nanostructures growth, enabling high-density aptamer immobilization via the 3D gold nanostructures architecture. This design achieved an LOD of 0.39 pg/mL across a dynamic range from 0.78 to 7.8×10^6 pg/mL in 10 min, demonstrating rapid and ultrasensitive thyroxine monitoring. These studies demonstrate the potential of nanomaterial-engineered electrochemical aptasensors to meet clinical needs for efficient thyroxine diagnostics, offering advantages in sensitivity, ease of operation, and real-time analysis compared to conventional techniques.

As a crucial biomarker of human metabolism, uric acid (UA) levels in body fluids can serve as direct indicators of metabolic and immune function [103]. Studies have demonstrated that abnormal UA levels are strongly linked to a variety of disorders, such as gout, hyperuricemia, cardiovascular diseases, and renal disorders [104]. Consequently, creating UA detection methods that are both highly sensitive and rapid holds significant clinical value. Ghanbari et al. [105] reported a novel electrochemical sensor by modifying a GCE with poly-L-cysteine, AuNPs, and B,N-co-doped reduced graphene oxide (Poly L-cys/AuNPs/B,N-rGO/GCE) for the concurrent monitoring of UA and xanthine (XA). This label-free sensor demonstrated excellent performance with wide linear ranges (3.0 nM to 3.0 μM for UA; 0.3 nM to 3.0 μM for XA), low detection limits (0.9 nM for UA; 90 pM for XA), and high sensitivities (1.908 $\mu A \cdot cm^{-2}\ \mu M^{-1}$ for UA; 0.846 $\mu A \cdot cm^{-2}\ \mu M^{-1}$ for XA). The sensor successfully quantified UA and XA in HS samples, providing advantages of simple preparation (via electrodeposition/electropolymerization), cost-effectiveness, and potential applicability for detecting other biomolecules.

In addition to the aforementioned cases, recent studies have made significant progress in sensing platforms for disease biomarker detection, as presented in Table 2. Overall, these results underscore the great promise of electrochemical aptamer sensors in enabling accurate identification of human biomarkers, thereby holding substantial value in improving diagnostic accuracy in clinical settings.

3.3. Hurdles in Clinical Translation

Despite the prominent advantages of electrochemical aptasensors in medical diagnostics, several critical challenges remain that hinder their clinical translation.

Table 2. Representative electrochemical aptasensor applications for disease biomarker detection.

Analyte	Electrode/Sensing Material	Disease Type	Electrochemical Method	Electrochemical Conditions (Electrolyte Solution; Reference Electrode)	LOD	Detection Range	Reference
Amyloid-β (42) oligomers	SnS_2 nanosheets	Alzheimer's disease (AD)	EIS	PBS (pH 7.4) + 5 mM $[Fe(CN)_6]^{3-/4-}$; -	238.9 fg/mL (PBS); 56.9 fg/mL (HS)	10^{-4}–10^3 ng/mL	[106]
Amyloid-β oligomers	Polyadenine/Gold electrode	AD	Linear Sweep Stripping Voltammetry	0.1 M KCl + 5 mM $[Fe(CN)_6]^{3-/4-}$; (saturated calomel electrode)SCE	430 fM	1 pM–10 nM	[107]
Hepatitis C virus core antigen	3D N-C@$NiCo_2O_4$ nanowire nanocomposite/GCE	Hepatitis C	EIS	5.0 mM $[Fe(CN)_6]^{3-/4-}$ + 0.1 M KCl; Ag/AgCl	0.16 fg/mL	0.5 fg/mL –0.12 pg/mL	[108]
P. falciparum histidine-rich protein II	Gold electrode	Malaria	SWV	PBS; Ag/AgCl	3.73 nM	-	[109]
p24-HIV protein	Graphene quantum dots/Screen-printed electrode (SPE)	Acquired immune deficiency syndrome	CV	PBS (0.1 M, pH 7.4) + 5 mM $[Fe(CN)_6]^{3-/4-}$; Ag/AgCl	51.7 pg/mL	0.93 ng/mL –93 pg/mL	[110]
Lactoferrin	Screen-printed gold electrode (SPGE)	Urinary tract infection	DPV	acetate buffer (0.1 M, pH 4.5); Ag	0.9 ng/mL	10 ng/mL–1300 ng/mL	[111]
cTnI	MoS_2/Cellulose acetate	AMI	EIS	PBS (pH 7.4) + 2 mM $[Fe(CN)_6]^{3-/4-}$; -	10 fM	10 fM–1 nM	[112]
cTnI	Hierarchical flower-like gold nanostructure/SPCE	AMI	SWV	PBS (0.01 M PB, 150 mM NaCl, pH 7.4); Ag/AgCl	8.46 pg/mL	10 pg/mL– 100 ng/mL	[113]
cTnI	Ferrocene-based covalent organic framework nanosheets/Gold electrode	AMI	DPV	PBS (10 mM, pH 6.86); Ag/AgCl	2.6 fg/mL	10 fg/mL–10 ng/mL	[114]
Interferon-Gamma	WS_2 nanotubes/nanocomposite conductive paper electrode	TB	DPV	PBS (0.1 M, pH 7.4) + 5 mM $[Fe(CN)_6]^{3-/4-}$; Ag/AgCl	1.13 pg/mL	3.125 pg/mL–100 pg/mL	[115]
CFP10-ESAT6	graphene/polyaniline/SPGE	TB	DPV	PBS (0.1 M, pH 7.4) + 5 mM $[Fe(CN)_6]^{3-/4-}$; Ag/AgCl	1.5 ng/mL	5 ng/mL–500 ng/mL	[116]
SARS-CoV-2 S-protein	AuNPs/Electrode	COVID-19	DPV	Tris-HCl buffer (pH 7.4); Ag/AgCl	91.1 pM	10 pM–6 nM	[117]
Serotonin	Gold electrode	Brain diseases	SWV	Low-salt PBS (pH 7.4); Ag/AgCl	0.14 nM	0.1 nM–1000 nM	[118]
Soluble CD80	AuSPE	Rheumatoid arthritis	EIS	PBS (pH 7.4) + 5 mM $[Fe(CN)_6]^{3-/4-}$; Ag/AgCl	8.0 pM	0.025 nM–10.0 nM	[119]
Calprotectin	High-Entropy Alloy Nanosheets/Amino acids	Inflammatory bowel disease	DPV	0.10 M KCl + 5 mM $[Fe(CN)_6]^{3-/4-}$; Ag/AgCl	2.02 pg/mL	5 pg/mL–100 ng/mL	[120]
C-reactive protein	Mercaptosuccinic acid-capped nickel selenide quantum dots	Myocardial infarction	Chronocoulometry	DPBS (10 mM, pH 7.4); -	2.80 pg/mL	10 pg/mL–110 pg/mL	[121]

Currently, researchers are devoted to enhancing the binding strength and recognition accuracy of aptamers for their target molecules through optimized aptamer design [122,123], yet numerous challenges remain. Primarily, the need to redesign specific sequences for different target analytes results in a time-consuming process for individual aptamer selection [124]. Secondly, the immobilization process onto the sensor surface, coupled with factors under physiological conditions including ionic strength, temperature, and pH fluctuations, can perturb the aptamer's conformational stability, leading to a reduction in binding affinity. For instance, Gabrusenok et al. studied the ATP aptamer and showed that its melting temperature and binding free energy (ΔG) depended on pH and Mg^{2+} concentration. At acidic pH, melting temperature decreased in the absence of Mg^{2+}, whereas ATP and Mg^{2+} modulated melting temperature differently depending on pH, illustrating that ionic conditions and protonation states can affect aptamer folding and binding stability [125]. Another study also showed that nine DNA aptamers examined in a fluorescence-encoded microbead multiplex assay exhibited reduced binding at higher ionic strength, loss of specificity at pH < 5, and modulation of binding by divalent cations (Ca^{2+}, Mg^{2+}, Mn^{2+}), indicating that environmental factors such as ion concentration and pH can significantly affect aptamer conformation and target affinity [126]. Finally, the complex matrix of real biological samples (e.g., urine, saliva, blood) can introduce interference. For instance, nonspecific binding of interfering proteins to the aptamer can occlude the recognition site for the target analyte (e.g., competitive adsorption by serum albumin), while free nucleic acids in biofluids can induce conformational changes in the aptamer upon binding [127–129]. For example, a study on electrochemical aptasensors showed that, in undiluted HS, the sensors exhibited an initial signal decrease of approximately 25% within the first 10 h, which was attributed to gradual desorption of both aptamers and blocking monolayer molecules, as well as nonspecific adsorption of serum proteins. This protein adsorption can sterically push aptamers closer to the electrode surface, altering electron-transfer kinetics and thereby interfering with sensor performance [130]. In addition, the study by Tsai et al. aimed to reduce signal drifts during long-term monitoring of structure-switching aptamers by using a dual-aptamer scheme, in which two ATP-binding aptamers signal differentially. Measurements in undiluted goat serum showed that both aptamers initially experienced signal drifts over time, but applying the differential signaling approach reduced the drift by several orders of magnitude. Nevertheless, variations in aptamer affinity, surface defects, and nonspecific interactions with serum components still influenced sensor performance, highlighting the challenges of using aptamer sensors in complex biological environments [131].

Furthermore, a significant gap remains between the performance of current sensors and the actual demands of clinical practice. Prevailing issues include poor short-term stability, lengthy incubation times, and low batch-to-batch reproducibility. Moreover, intrinsic challenges in disease diagnostics further complicate this landscape: first, certain diseases, such as multiple sclerosis, lack highly specific biomarkers; second, the accurate diagnosis of many conditions relies on the concurrent assessment of several biomarkers—for instance, cardiac infarction requires the combined measurement of cTnI, myoglobin, and creatine kinase-MB isoenzyme. In the case of highly heterogeneous diseases such as cancer, diagnostic strategies relying on a single biomarker often suffer from insufficient specificity and limited accuracy. Compounding these issues, technical barriers hinder reliable multiplexed detection: electrochemical cross-talk between channels not only constrains the throughput for multi-analyte sensing but also increases the risk of cross-reactivity.

A final critical challenge on the path to clinical translation is that current research on aptasensors predominantly relies on idealized spiked samples or in vitro models, lacking comprehensive evaluation of the matrix effects inherent in complex clinical samples. To

date, research using genuine human samples remains limited. Therefore, a key focus of future work must be the systematic assessment of sensor sensitivity and accuracy in realistic clinical environments containing high levels of interferents—an essential step toward clinical translation [132].

4. Application of Electrochemical Aptasensors in Food Inspection

Food safety, which is closely intertwined with population health, has attracted increasing global attention. The presence of toxic agents such as pathogens, antibiotics, pesticide residues, mycotoxins, and heavy metal ions is a primary cause of foodborne diseases [133–135]. These contaminants can enter the food chain at various stages, including excessive agrochemical use in agriculture, polluted soil and water, microbial growth during storage, and cross-contamination in processing and transportation. Accurate detection of these hazards is crucial for disease prevention. However, conventional methods, including chromatography, mass spectrometry, and fluorescence techniques, have inherent limitations [136,137]. The complex and variable composition of food matrices poses significant challenges for developing efficient detection technologies. Consequently, electrochemical aptamer sensors, renowned for their excellent sensitivity, selectivity, and operational simplicity, are considered promising candidates for next-generation food safety diagnostic solutions.

4.1. Electrochemical Aptasensors for Antibiotic Detection

Antibiotics, a class of antimicrobial metabolites, are widely used in disease treatment and animal growth promotion. Nevertheless, their overuse results in bioaccumulation in people via dietary exposure, making the quantitative detection of antibiotic residues in animal-derived foods essential for public health [138]. Malecka-Baturo et al. [139] reported an electrochemical biosensor employing the conjugation of ferrocene and ssDNA aptamer. The sensor utilizes a tetracycline-specific thiolated ssDNA aptamer covalently immobilized on a Au electrode with 6-mercaptohexanol. The redox behavior of ferrocene is influenced by the interaction of the aptamer with the antibiotic, and the signals are recorded via SWV. The device achieved LODs of 0.16 nM in buffer and 0.20 nM in spiked milk samples, demonstrating high selectivity and practical utility for tetracycline monitoring. Wei et al. [140] developed a novel platform for ampicillin detection. The platform features electrospun Bi_2O_3 nanomaterials as the substrate and AuNPs conjugated to 5′-thiolated aptamers, enabling stable immobilization of Bi_2O_3-aptamer complexes. DPV analysis shows that the peak currents decrease with rising ampicillin levels, exhibiting an LOD of 0.88 nM and a linear range of 1 nM to 10 mM. The sensor successfully detected ampicillin residues in water and milk samples, highlighting its applicability in food safety diagnostics.

A recent investigation introduced an electrochemical biosensor for the aminoglycoside antibiotic kanamycin [141]. The functional surface was constructed by self-assembling a kanamycin -specific DNA aptamer and its complementary oligonucleotides onto a portable plastic gold electrode via Au-S bonding. An epoxy resin microchannel layer was integrated to enable sequential analysis of eight samples, achieving a linear detection range of 1 to 1000 μmol/L and an LOD of 0.40 μmol/L. This configuration demonstrated rapid response kinetics and operational stability, providing a robust platform for kanamycin screening. A label-free electrochemical aptasensor for detecting oxytetracycline (OTC), a widely used antibiotic, was introduced by Akbarzadeh et al. [142]. The sensor employed OTC-specific aptamers immobilized on GCEs modified with hierarchical nanocomposites of multiwalled carbon nanotubes (MWCNTs), rGO, chitosan, and AuNPs. Constructed through a layer-by-layer assembly process (MWCNTs-AuNPs/chitosan-AuNPs/rGO-AuNPs), this architecture enhanced aptamer stability and electron transfer kinetics. The aptasensor

exhibited an LOD of 30.0 pM and a linear range of 1.00 to 540 nM in milk samples, with exceptional repeatability, reproducibility, and resistance to structural analog interference, establishing its utility for OTC monitoring in complex matrices.

Collectively, the aforementioned studies highlight the potential of electrochemical aptamer biosensors for monitoring antibiotic residues in food. While most reports are still at the laboratory validation stage, these sensors have been evaluated in spiked or real food samples such as milk and water, demonstrating promising sensitivity and selectivity.

4.2. Electrochemical Aptasensors for Mycotoxin Detection

Mycotoxins, which are harmful secondary metabolites generated by fungal species, contaminate the food chain through diverse pathways. Common foodborne mycotoxins include aflatoxins, trichothecenes, fumonisins, and ochratoxin, among others [143]. Ingesting food or feed tainted with mycotoxins may lead to both acute and long-term toxic effects in humans and animals. Aflatoxin M1, the milk-excreted hydroxylation product formed from aflatoxin B1, is primarily found in dairy products, exhibiting hepatotoxic and carcinogenic potential. Stringent regulatory limits for aflatoxins in food are enforced globally [144,145]. Yang et al. [146] reported a novel sensor integrating electrochemical molecularly imprinted polymer with aptamer-mediated signal amplification for Aflatoxin M1 quantification in milk. The dual-recognition architecture, incorporating molecularly imprinted polymer and Apt via Au-S bonding and electropolymerization onto an AuNPs-modified GCE, significantly enhanced detection sensitivity. Under optimized conditions, the platform displayed a linear range of 0.01 to 200 nM with an LOD of 0.07 nM. This study represents the first report of Aflatoxin M1 detection using dual-recognition signal amplification, offering a novel paradigm for toxin analysis. However, while the sensor demonstrated good sensitivity and selectivity under controlled conditions, the manuscript does not address the potential impact of complex matrices (such as fat and protein in milk) on sensor performance. Therefore, further validation in real, unprocessed samples is needed.

Designing dual signal amplification mechanisms in sensors significantly enhances detection sensitivity, as demonstrated by a recent study [147] that developed a biosensor for ochratoxin A, a mycotoxin generated by *Aspergillus* and *Penicillium* species, contaminating foods such as red wine, milk, coffee, grains, and spices [148–150]. The sensor employs a two-tier amplification strategy: silver nanoparticles (AgNPs) increase aptamer loading on the electrode surface to enhance ochratoxin A capture (primary amplification), while a PEI-modified ochratoxin A antibody forms an aptamer-ochratoxin A-antibody sandwich structure. The amino groups of PEI initiate the ring-opening polymerization of α-amino acid-N-carboxylic anhydride-ferrocene, introducing numerous ferrocene units for secondary electrochemical signal amplification. With optimized parameters, the sensor achieves a detection range of 1 pg/mL to 1 μg/mL with an LOD of 117 fg/mL, showcasing both high sensitivity and excellent stability/selectivity. However, the sensor also lacks further testing in more complex, unprocessed samples to assess its robustness in real-world applications.

4.3. Electrochemical Aptasensors for Foodborne Pathogens Detection

Food safety issues are significantly affected by foodborne pathogens, which contaminate food during production and transportation. Representative pathogens include *Salmonella*, *Staphylococcus aureus* (*S. aureus*), *Clostridium perfringens*, *Listeria monocytogenes*, *Shigella* spp., and *Campylobacter jejuni* [151–153]. Ingestion of contaminated food allows these pathogens to trigger foodborne diseases. According to the World Health Organization, 31 major foodborne pathogens are responsible for an estimated 600 million cases and

420,000 deaths worldwide each year [154]. Therefore, effective detection of these pathogens is a key strategy to mitigate public health risks.

S. aureus is a prominent foodborne pathogen commonly present in high-protein matrices, particularly meat and dairy products. This bacterium is a leading etiological agent of respiratory infections, sepsis, cardiovascular infections, pneumonia, nosocomial bacteremia, surgical site infections, and other diseases [155]. Current detection methods for *S. aureus*, such as bacterial culture, PCR, and immunoassays, have inherent limitations. The gold-standard culture method, although highly accurate, has long incubation times, underscoring the pressing demand for diagnostic methods with higher sensitivity and efficiency [156,157]. Hui et al. [158] developed a sandwich-format electrochemical aptasensor for *S. aureus* detection. The sensor was fabricated by first drop-coating a GCE with AgNPs -embedded titanium carbide nanocomposites (AgNPs@Ti_3C_2). Aptamers specific to *S. aureus* were assembled onto the modified electrode, and biocompatible copper oxide/graphene nanocomposites served as signal probes for aptamer immobilization. In the presence of the target pathogen, copper oxide/graphene nanocomposites catalyze the oxidation of hydroquinone to benzoquinone using H_2O_2, generating a strong electrochemical response. Under optimal conditions, the sensor achieved an LOD as low as 1 CFU/mL and successfully detected *S. aureus* in bovine, sheep milk, and goat samples, indicating its promising application in pathogenic pathogen detection. Nguyen et al. [159] reported the development of homologous aptamer pair SA37 (primary aptamer) and SA81 (secondary aptamer) that simultaneously bind to *Staphylococcus aureus*. SA37 serves as a capture fragment, while SA81 functions as a signaling aptamer, both exhibiting high affinity for *S. aureus*. The aptamers were immobilized on a SPGE to construct a sandwich-type electrochemical aptasensor, enabling specific dual binding to the target pathogen. The sensor achieved LODs of 39 CFUs in buffer solution and 414 CFUs in tap water, demonstrating benefits such as ease of operation, affordability, and high sensitivity. Appaturi et al. [160] designed an electrochemical aptamer sensor for rapid *Salmonella enterica* detection, constructed from rGO-CNT nanocomposites prepared through a hydrothermal method. The nanocomposites were deposited onto a GCE and then modified with amino-functionalized DNA aptamers. DPV was employed to detect bacteria using the fabricated ligand sensor. Under optimized experimental conditions, the sensor demonstrated a linear detection range of 10^1 to 10^8 CFU/mL for *Salmonella typhimurium*, with an LOD of 10^1 CFU/mL. The sensor demonstrated excellent selectivity, sensitivity, and specificity in detecting *Salmonella typhimurium* in real food samples.

The three studies mentioned above share a common goal of developing aptamer-based biosensors for detecting *Staphylococcus aureus* and *Salmonella* enterica, but they all face similar limitations. These include the reliance on complex and costly preparation methods like SELEX and hydrothermal synthesis for nanocomposites, which can hinder scalability and affordability for broader use in food safety. While the biosensors show good sensitivity and stability in controlled environments, their practical application in diverse food matrices and environments is still uncertain, highlighting the need for further evaluation to confirm their true effectiveness in food safety management. In addition to the cases described above, Table 3 summarizes additional reported instances of electrochemical aptamer sensors for foodborne pathogen detection from recent years.

Table 3. Representative electrochemical aptasensor applications for foodborne pathogen detection.

Analyte	Biosensor Used	Food Category	Electrochemical Method	Electrochemical Conditions (Electrolyte Solution; Reference Electrode)	LOD	Detection Range	Reference
Escherichia coli O157:H7	Au-nanoparticle-modified GCE	Penaeus vannamei samples	EIS	PBS (0.01 M, pH 7.0) + 5 mM $[Fe(CN)_6]^{3-/4-}$; Ag/AgCl	4.0 CFU/mL	1.5×10^1 CFU/mL–1.5×10^5 CFU/mL	[161]
E. coli	AgNP-modified SPCE	Tap water samples	DPV	PBS (10 mM, pH 7.4) + 2.5 mM $[Fe(CN)_6]^{3-/4-}$; Ag/AgCl	150 CFU/mL	-	[162]
S. aureus	mixed ligands-Cu_2O@Cu-MOF	Milk, honey, and biscuit	EIS/DPV	PBS (0.1 M, pH 7.4)+ 0.5 mM $[Fe(CN)_6]^{3-/4-}$ + KCl (1 M); Ag/AgCl	2 CFU/mL (EIS)/16 CFU/mL (DPV)	10 CFU/mL–1×10^8 CFU/mL	[163]
S. aureus	Gold electrode	Water samples and honey samples	DPV	PBS (pH 7.4); Ag/AgCl	9 CFU/mL	60 CFU/mL–6×10^7 CFU/mL	[164]
Micrococcal nuclease (*S. aureus* biomarker)	Gold electrode	Spiked milk samples	DPV	0.1 M KCl + 3 mM $[Fe(CN)6]^{3-/4-}$; Ag/AgCl	2.37×10^{-5} U/μL	0.00022 U/μL–0.02 U/μL	[165]
S. aureus	AuNPs@Zeolitic imidazolate framework (ZIF)	Orange juice and milk samples	DPV	-	1 CFU/mL	5 CFU/mL–10^8 CFU/mL	[166]
S. aureus	GCE/ZIF-8/AuNPs	Water and milk samples	EIS	PBS (0.1 M, pH 7.4) + 5 mM $[Fe(CN)_6]^{3-/4-}$ + 1 M KCl, Ag/AgCl	3.4 CFU/mL	1.5×10^1 CFU/mL–1.5×10^7 CFU/mL	[167]
Norovirus	Carbon ink/Black phosphorene–Gold nanocomposites	Oyster samples	DPV	0.1 M KCl + 5 mM $[Fe(CN)_6]^{3-/4-}$); Ag/AgCl	0.28 ng/mL	1 ng/mL–10 μg/mL	[168]
Norovirus	AuNPs/GCE	Spiked oysters, strawberries, and fecal samples	DPV	PBS, -	0.84 copy/mL	-	[169]
Vibrio parahaemolyticus	SPE	Shrimps	SWV	-	5 CFU/mL	10 CFU/mL–10^8 CFU/mL	[170]
Listeria monocytogenes	Tungsten disulfide-modified electrochemical paper-based analytical device	Dairy products	EIS	0.1 M KCl + 0.1 mM MB	10.0 CFU/mL	10^1 CFU/mL–10^8 CFU/mL	[171]
Listeria monocytogenes	Alginate-thiomer/Pt nanobrush	Chicken broth	EIS	Sample itself (PBS or food matrix); Ag/AgCl	5 CFU/mL	10^1 CFU/mL–10^6 CFU/mL	[172]
Salmonella enteritidis	AuNPs/GCE	Penaeus vannamei	EIS	5 mM $[Fe(CN)_6]^{3-/4-}$; Ag/AgCl	20.704 CF/mL	6×10^1 CFU/mL–6×10^5 CFU/mL	[173]
aflatoxin B1	AuPt-Ru/rGO/Gold leaf electrode	Dried red chili, garlic, peanuts, pepper and Thai jasmine rice	DPV	PBS (20 mM, pH 7.0) + 5 mM $K_3[Fe(CN)_6]$; Ag/AgCl (3.5 M KCl)	9×10^{-3} pg/mL	0.3–30.0 pg/mL	[174]

4.4. Electrochemical Aptasensors for Insecticide Residue Detection

Insecticides are indispensable in crop cultivation, effectively controlling pests and enhancing agricultural productivity and product quality, thereby meeting the food demands of the growing global population [175]. However, their extensive application for pest management and yield improvement has led to persistent pesticide residues, posing significant health risks to humans [176]. Aerosolized pesticides absorbed by clouds contaminate atmospheric, aquatic, and terrestrial ecosystems through rainfall. Their environmental persistence enables bioaccumulation in the food chain, and studies have demonstrated their cytotoxic effects and carcinogenic potential [177]. Consequently, establishing reliable and sensitive analytical approaches for monitoring pesticide residues in food is essential to mitigate these risks.

Malathion is a widely used organophosphate pesticide. Its residues contaminate water systems and pose significant health risks, thereby necessitating efficient detection methods for malathion residues [178]. Ma et al. [179] reported a label-free electrochemical sensing platform based on hydroxylated black phosphorus/poly-L-lysine (hBP/PLL) nanocomposites, enabling sensitive malathion analysis. The hBP/PLL composites were first formed via non-covalent interactions and then immobilized onto AuNPs-modified GCEs. This architecture not only enabled binding of malathion-specific aptamers but also improved sensing response. After optimizing the aptamer–malathion incubation time (saturation reached at 40 min), this platform exhibited a linear range of 0.1 pM to 1 μM and an LOD as low as 2.805 fM, demonstrating its high sensitivity for malathion detection in food matrices.

Given the complexity and diversity of pesticides in use, researchers have focused on developing biosensors for multi-pesticide detection. Wang et al. [180] developed a bimodal sensor based on single-atom iron nanozyme for detecting multiple organophosphorus compounds. The single-atom iron nanozyme catalyzes the oxidation of 3,3′,5,5′-tetramethylbenzidine (TMB) to generate the blue product TMBox. Meanwhile, organophosphorus pesticides binding to aptamers on the single-atom iron nanozyme surface form complexes that inhibit nanozyme activity, blocking TMB oxidation. Concurrently, the MB-labeled complexes approach the electrode surface due to conformational changes, inducing electrochemical signal variations. Under optimized conditions, this broad-spectrum aptasensor achieved a detection limit of 3.55 fM and a linear range of 1×10^{-13} to 1×10^{-2} M. The integration of colorimetric and electrochemical detection modalities enhanced both accuracy and sensitivity. Building on the previous summary, the dual-mode biosensor shows significant potential but has some key limitations as acknowledged by the authors. The sample pre-processing is overly cumbersome, requiring a large amount of reagents, which increases the cost of the biosensor. Additionally, while the dual-mode approach enhances accuracy and sensitivity, existing smartphones lack electrochemical detection capabilities and can only accommodate colorimetric methods. The authors suggest that external electrochemical devices compatible with smartphones are needed for full multimodal detection, highlighting the need for further innovation in portable detection technology.

4.5. Challenges in Food Inspection

Despite their promising application potential in food safety monitoring, electrochemical aptasensors still face several critical limitations. A primary challenge stems from complex food matrices (e.g., milk, meat, fruit juices), where proteins, fats, and structurally analogous components can cause non-specific binding, false-positive signals, and signal suppression [181]. Secondly, when trace contaminants (e.g., mycotoxins, antibiotics) are present at low concentrations or unevenly distributed in authentic samples, low extraction efficiency may lead to false-negative results [182]. Furthermore, the physicochemical pa-

rameters of food samples, such as viscosity, storage temperature, and pH, exhibit significant variations depending on their sources, batches, and processing methods, making it difficult to adopt a uniform detection standard [183].

Several approaches have been explored to address these challenges. To mitigate cross-reactivity and false positives resulting from interference in complex food matrices, a variety of sample pretreatment methods are commonly utilized, including centrifugation, dilution [184], organic solvent extraction [185] and immunomagnetic separation [186], among others. Furthermore, during the aptamer screening phase, a series of optimization strategies can be employed, including high-pressure cross-screening (which applies high selection pressure through structural analogs and low target concentrations) [187] and chemical modifications [188]. These approaches aim to obtain aptamers with high selectivity, strong affinity, and excellent matrix adaptability [181]. Another promising solution is the integration of multimodal detection systems, combining aptamers with complementary techniques (e.g., spectroscopy or colorimetric methods) to improve specificity and sensitivity in complex matrices.

Future studies will focus on standardizing analytical protocols and improving sensor reliability for complex food matrices. Specifically, there is an urgent need for more robust sample preparation technologies that can easily adapt to different food products. Moreover, the development of portable devices that integrate electrochemical detection with smartphone-assisted analysis will facilitate the transition from laboratory platforms to field-deployable, rapid monitoring applications [189,190].

5. Application of Electrochemical Aptasensors in Monitoring of Environmental Hazards

Environmental contaminants, including industrial chemicals, biological toxins, and toxic heavy metals, are widely distributed in air, water, and soil due to anthropogenic activities [191,192]. These pollutants can bioaccumulate through food chains and pose significant risks to ecosystems and human health. This highlights the urgent need for sensitive and rapid environmental monitoring tools. In response, electrochemical aptasensors have demonstrated good selectivity and rapid response in experimental studies and have been investigated for detecting trace-level environmental pollutants.

5.1. Heavy Metal Detection

Residual heavy metals from industrial and agricultural activities infiltrate atmospheric, soil, and aquatic environments. Their accumulation in soil threatens crop yields, water resources, and human health through food chain bioaccumulation [193]. Ding et al. [194] reported an electrochemical aptasensor for soil Pb^{2+} detection by immobilizing the Pb^{2+}-specific aptamer complementary strands via hybridization onto AuNPs-polypyrrole composites. The aptamer recognition element was constructed via complementary strand hybridization, using toluidine blue as a redox indicator. Validated by CV and DPV, the device demonstrated a linear range of 0.5 to 25 ppb for Pb^{2+} under optimal conditions, with a detection limit of 0.6 ppb. Its good reproducibility allowed effective Pb^{2+} analysis in soil samples, highlighting its applicability in environmental monitoring. Gao et al. [195] reported an aptasensor capable of detecting both Pb^{2+} and Hg^{2+} by attaching two distinct aptamers onto a gold electrode (Figure 5). The sensor utilized melamine–Cu^{2+} complex and Nile blue as signal tags, grafted in situ onto the termini of Pb^{2+}- and Hg^{2+}-binding aptamers to form a dual-signal interface. The presence of redox tags with distinct potentials generated two independent redox peak pairs during detection. The LODs for Pb^{2+} and Hg^{2+} were 0.98 pM and 19 pM, respectively, with successful application to real water sample analysis. While both studies acknowledge the advantages of electrochemical ap-

tasensors over traditional methods, they are limited by the need for specialized equipment, such as electrochemical workstations and screen-printed electrodes, which are not widely accessible for routine field monitoring.

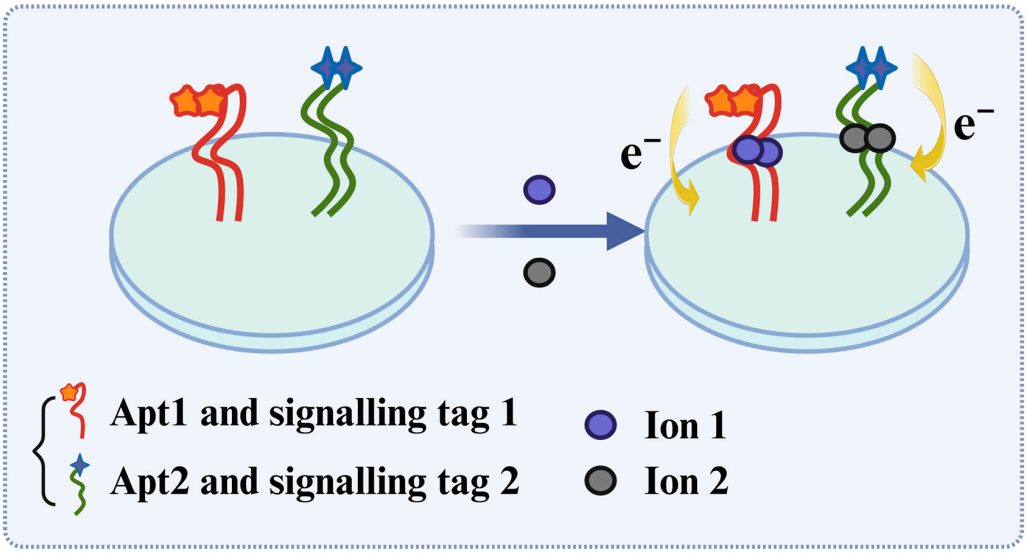


Figure 5. Brief structure of an electrochemical aptasensor capable of simultaneous detection of two heavy metals. The illustration was created by using BioRender (web version; https://biorender.com).

5.2. Detection of Harmful Compounds

Industrial activities inevitably generate toxic compounds that, if unregulated, persist in water, soil, and atmospheric environments, causing ecological damage. Bisphenol A (BPA), a key industrial monomer used in polycarbonate and epoxy resin synthesis, has been detected in dust, airborne particles, and aquatic systems, posing endocrine-disrupting risks to biological organisms [196]. To address trace BPA detection, researchers developed an electrochemical sensing platform based on bimetallic AgMo heterostructures (Ag-PMo_{12}) [197]. The platform was synthesized by hydrothermal doping of silver ions into phosphomolybdic acid followed by temperature-controlled annealing. Calcination of Ag-PMo_{12} at 600 °C yielded nanohybrids comprising Ag, Ag_2O, Ag_2S, and ultrathin MoS_2 nanosheets, which exhibited excellent biocompatibility, electrochemical activity, and strong aptamer adsorption capacity. Notably, MoS_2 nanosheets serve as a high-surface-area support to suppress aggregation of Ag-based nanocrystals, while the coexistence of Ag, Ag_2O, and Ag_2S provides multiple valence states that can interact with different functional groups of DNA. This synergistic architecture facilitates electron transfer and aptamer anchoring, thereby contributing to signal amplification. Consequently, the aptamer-functionalized nanohybrids enabled sensitive BPA detection via target-induced conformational changes, achieving a linear range of 1 to 1000 fg/mL and a detection limit of 0.2 fg/mL. This platform combines indicator-free operation, intrinsic signal amplification, and high selectivity and stability, providing a valuable approach for environmental BPA monitoring.

Diclofenac (DCF), a common non-steroidal anti-inflammatory agent, infiltrates aquatic and soil ecosystems through industrial wastewater and veterinary excretion, posing significant risks to ecological safety [198]. Zou et al. [199] designed an aptasensor for trace DCF analysis, employing DCF-specific aptamers as biorecognition elements covalently immobilized on GCEs modified with carboxyl-functionalized MWCNTs. The carboxyl-functionalized MWCNT platform enabled high-density aptamer immobilization, facilitating specific binding to DCF and formation of DCF-aptamer complexes. EIS was used to monitor Rct changes induced by complex formation. The sensor exhibited two linear

ranges: 250 fM to 1 pM and 1 pM to 500 nM, with an LOD as low as 162 fM. Featuring excellent reproducibility, stability, and selectivity, this biosensor offers a convenient strategy for DCF quantification in environmental matrices, demonstrating promising utility in ecological quality monitoring

Both the BPA and DCF aptasensors show promising sensitivity and specificity for environmental monitoring. However, their reliance on specialized equipment still limits their practical field application.

5.3. Detection of Biotoxins

Numerous flora and fauna produce bioactive toxins during ontogenesis, which pose environmental contamination risks when entering ecosystems. Notably, microcystins, secondary metabolites synthesized by cyanobacteria, are ubiquitously detected in cyanobacterial blooms. In recent decades, the increasing prevalence of harmful algal blooms, driven by eutrophication and climatic changes, has exacerbated water contamination by microcystins [200].

Microcystin-LR, the most potent microcystin variant, requires sensitive in situ detection in aquatic environments. Wang et al. [201] designed an electrochemical aptasensor based on a laser-induced graphene (LIG) electrode, acting as a quasi-reference electrode and functionalized with AuNPs, providing a relatively stable potential for current-based measurements without using a conventional Ag/AgCl reference electrode, thus facilitating rapid fabrication and on-site detection. TDNs conjugated with high-affinity aptamers (TDNs-cDNA-aptamer complexes) were synthesized via PCR and assembled onto the LIG electrode through Au-S bonding. The high surface area of LIG enables dense TDNs assembly, with MB adsorbed as a redox indicator. Upon Microcystin-LR binding, the TDNs complex dissociates, reducing MB-mediated redox current. The sensor demonstrates a linear response from 1×10^{-2} to 1×10^{5} pM, with an LOD of 3×10^{-3} pM, effectively applied to in situ analysis of environmental water samples with excellent reproducibility. Saxitoxin, a paralytic shellfish toxin and one of the most potent marine biotoxins, was detected using an electrolyte-insulator-semiconductor sensor developed by Noureen et al. [202]. The sensor features a positively charged weak polyelectrolyte layer (poly(allylamine hydrochloride)) for electrostatic adsorption of saxitoxin-specific aptamers. This architecture enables label-free detection via aptamer–saxitoxin binding-induced surface charge changes. The platform demonstrates a detection range of 0.5 to 100 nM with an LOD of 0.05 nM, showcasing high selectivity and stability in real seawater samples. Its performance highlights potential for on-site monitoring of marine biotoxins.

Research on electrochemical aptasensors applied more extensively in environmental pollutant detection is presented in Table 4, highlighting their potential as a promising and versatile platform for next-generation environmental monitoring.

Table 4. Representative applications for environmental hazard detection.

Analyte	Key Electrode Material	Sample	Primary Electrochemical Methods	Electrochemical Conditions (Electrolyte Solution; Reference Electrode)	LOD	Detection Range	Reference
2,4,6-Trinitrotoluen	Microstructure porous-covalent organic polymer/GCE	Harmful compounds	DPV	0.1 M KCl + 5 mM $[Fe(CN)_6]^{3-/4-}$; Ag/AgCl	0.0003 pM	0.001 pM–100 pM	[203]
Erwinia cypripedii	rGO-Nitrogen-doped Carbon derived from ZIF-8	Biological hazard	DPV	5 mM $[Fe(CN)6]^{3-/4-}$ in 0.1 M KCl; Ag/AgCl	4.92×10^3 CFU/mL	2×10^5–2×10^9 CFU/mL	[204]
Pb^{2+}	Gold electrode/SPE	Heavy metals	SWV	50 μM MB in 50 mM Tris-HCl; pH 4.0, Ag/AgCl	21 nM	10 nM–100 nM	[205]
Dibutyl phthalate	Epoxy-functionalized magnetic nanoparticles	Harmful compounds	EIS	5 mM $[Fe(CN)_6]^{3-/4-}$ in 1 M KCl; Ag/AgCl	0.32 pg/mL	1–200 pg/mL	[206]
Carbendazim	Carbonized and Oxidized Eggshell Membranes	Harmful compounds	DPV	5 mM $[Fe(CN)_6]^{3-/4-}$ in 0.1 M PBS (pH 7.4) with 0.1 M KCl; Ag/AgCl	0.686 μg/L	0.19 μg/L–11.47 μg/L	[207]
BPA	Gold electrode	Harmful compounds	SWV	25 mM Tris-HCl (pH 8.0) + 100 mM NaCl + 25 mM KCl + 10 mM $MgCl_2$; Ag/AgCl (3 M KCl)	0.1 μM	0.1 μM–10 μM/ 10 μM–1000 μM	[208]
Lincomycin and neomycin	SPCE/AuNPs/Carbon nanofibers	Antibiotic	SWV	PBS (10 mM, pH 7.4) + 5 mM $K_4Fe(CN)_6/K_3Fe(CN)_6$; Ag	0.02 pg/mL and 0.035 pg/mL	0.01 pg/mL–1 μg/mL	[209]
Profenofos and diazinon	C-MWCNTs@Fe_3O_4 NPs/AuNPs/DNA tetrahedral scaffold	Pesticides	DPV	1 M acetate buffer (pH 7); –	3.33 pg/mL	1.00×10^1 pg/mL– 1.00×10^7 pg/mL	[210]
Acetamiprid	rGO-AgNPs/Prussian blue-AuNPs/GCE	Pesticides	CV	0.01 M PBS + 5 mM $[Fe(CN)_6]^{3-/4-}$ + 0.1 M KCl; SCE	0.30 pM	1 pM–1 μM	[211]

5.4. Application Challenges in Environmental Monitoring

Despite these advancements, their translation from laboratory research to practical field applications remains fraught with challenges.

The first challenge lies in the inherent limitations of aptamers. Taking pesticide residue detection as an example, the mechanistic studies of aptamers in pesticide molecule detection remain insufficient. Current analyses primarily focus on the characterization of aptamer secondary structures [212]. However, the vast diversity and structural similarities among pesticides pose significant challenges. The availability of pesticide-specific aptamers is still limited; existing aptamer-based detection methods can target only approximately 20 pesticides, representing a small fraction of the hundreds of known pesticide variants. This constraint in the aptamer repertoire severely restricts the broad-spectrum detection capability of aptasensors for multiple pesticide residues in complex samples [213].

Secondly, although the number of reported aptasensors for detecting toxic chemicals has increased rapidly in recent years, successful detection of aptamer ligands in environmental samples remains limited. Compared to biological matrices (e.g., blood), water—as a primary medium in environmental monitoring—exhibits lower compositional complexity. Nevertheless, in situ monitoring of contaminants in aquatic environments still faces notable technical challenges. These primarily stem from non-specific interactions and competitive binding caused by abundant coexisting molecules in environmental samples. Moreover, unlike medical laboratories equipped with stable power supply and refrigeration, environmental sample collection and storage are often conducted in outdoor settings with fluctuating temperature and humidity, significantly compromising detection reliability [214,215].

Furthermore, most reported systems are designed for single-target detection, without the simultaneous detection capability required for comprehensive environmental monitoring. Additionally, lack of standardized fabrication protocols and regulatory guidelines for aptamer-based devices significantly hinders their deployment in environmental applications. The current sensor fabrication relies on molecule-specific customization without unified standards, severely limiting their practical utility for on-site environmental monitoring and commercial viability [216].

6. Conclusions and Perspective

Electrochemical aptasensors have achieved remarkable advancements for biomedical, food safety, and environmental applications, harnessing the synergistic advantages by integrating the unique properties of aptamer recognition (high selectivity/stability) and electrochemical detection (sensitivity, cost-effectiveness). Notably, their applications in medical fields show considerable promise for early clinical diagnosis and therapeutic efficacy monitoring. These sensors have been successfully incorporated into wearable devices, enabling continuous health tracking via mobile connectivity. In food safety monitoring, they efficiently detect various contaminants, including pathogens, biotoxins, pesticides, and heavy metals. Meanwhile, their applications in environmental pollutant detection and industrial fields have also demonstrated promising prospects. Technological progress in this field is fundamentally driven by interdisciplinary research, which focuses on integrating aptamers with nanomaterials (e.g., graphene, metal nanoparticles) to optimize sensor performance. This approach has significantly enhanced detection accuracy and operational stability. Nonetheless, a number of challenges still need to be tackled: the current repertoire of aptamer-targeted analytes is still limited, requiring expanded sequence screening via advanced SELEX strategies; meanwhile, interferences from complex matrices in real-world samples necessitate the development of advanced anti-interference mechanisms. Despite

these challenges, electrochemical aptasensors are poised to evolve into ideal detection platforms for various applications.

Looking forward, the real-world applications of electrochemical aptasensors will continue to expand significantly. For example, in biomedical diagnostics, we can expect more sophisticated sensors capable of simultaneously detecting multiple disease biomarkers in point-of-care settings, which will play a key role in personalized medicine. In food safety, there is a growing demand for portable, low-cost devices for on-site detection of a wide range of contaminants, such as pesticide residues in agricultural products, contributing to food safety assurance throughout the supply chain. Environmental monitoring will also benefit from advancements in sensor technology, leading to the development of miniaturized, cost-effective systems for detecting pollutants, including heavy metals in water sources and air quality monitoring, deployable even in remote areas with limited laboratory resources.

Continued innovation in aptamer engineering and nanomaterial design will further drive these technological advances, enhance sensor performance, and accelerate the widespread adoption of these sensors as routine diagnostic tools in clinical, food safety, and environmental monitoring fields.

Author Contributions: All authors contributed to the study conception and design. Writing—original draft preparation, Visualization, Investigation and Data collection: W.S. and P.Z.; Data collection, Investigation: M.L., G.L. and M.S.; Conceptualization, Writing—review and editing, Supervision, and Project administration: X.M. and Y.L. All authors commented on previous versions of the manuscript. All authors have read and agreed to the published version of the manuscript.

Funding: This research was supported by the Natural Science Foundation of Shandong Province, grant number ZR2021MH146, the Medicine and Health Science and Technology Development Plan Project of Shandong Province, grant number 202012060616, the College Students' Innovation and Entrepreneurship Training Program Project of Shandong Province, grant number S202510438063, the Natural Science Foundation of Fujian Province, grant number 2024J011175, the Research Project of Fashu Foundation, grant number MFK25017.

Informed Consent Statement: Informed consent was not required for this review.

Data Availability Statement: Not applicable.

Conflicts of Interest: The authors declare no conflicts of interest.

Abbreviations

SELEX	Systematic Evolution of Ligands by Exponential Enrichment
MB	Methylene Blue
CV	Cyclic Voltammetry
DPV	Differential Pulse Voltammetry
SWV	Square Wave Voltammetry
EIS	Electrochemical impedance spectroscopy
Rct	Charge Transfer Resistance
CA	Chronoamperometry
ENOX2	Ecto-NOX disulfide-thiol exchanger 2
LOD	Limit of Detection
EpCAM	Epithelial Cell Adhesion Molecule
TDNs	Tetrahedral DNA Nanostructures
RCA	Rolling Circle Amplification
SMRT	Split Aptamer-mediated Regenerative Temperature-sensitive
PBS	Phosphate-Buffered Saline
PD-L1	Programmed Death Ligand 1

HER2	Human Epidermal Growth Factor Receptor 2
AuSPE	Gold Screen-printed Electrode
SAM	Self-assembled Monolayer
MCH	1-mercapto-6-hexanol
HDT	1,6-hexanedithiol
HS	Human Serum
PCa	Prostate Cancer
PSA	Prostate-specific Antigen
MoS2	Molybdenum Disulphide
CEA	Carcinoembryonic Antigen
GCE	Glassy Carbon Electrode
SPCE	Screen-printed Carbon Electrode
AFP	Alpha-fetoprotein
TB	Tuberculosis
MTB	*Mycobacterium tuberculosis*
ESAT-6	Early Secreted Antigenic Target 6
H. pylori	*Helicobacter pylori*
CVDs	Cardiovascular Diseases
AMI	Acute Myocardial Infarction
cTnI	Troponin I
CNT	Carbon Nanotube
EOCV	Open-circuit Voltage
IFN-γ	Interferon-γ
IL-6	Interleukin-6
TNF-α	Tumor Necrosis Factor-α
ACEF	Alternating Current Electrothermal Flow
MOF	Metal–organic Framework
UA	Uric Acid
XA	Xanthine
AD	Alzheimer's Disease
SPE	Screen-printed Electrode
SPGE	Screen-printed Gold Electrode
OTC	Oxytetracycline
MWCNTs	Multi-walled Carbon Nanotubes
AgNPs	Silver Nanoparticles
ZIF	Zeolitic Imidazolate Framework
TMB	3,3′,5,5′-tetramethylbenzidine
DCF	Diclofenac
LIG	Laser-induced Graphene

References

1. Grieshaber, D.; MacKenzie, R.; Vörös, J.; Reimhult, E. Electrochemical Biosensors—Sensor Principles and Architectures. *Sensors* **2008**, *8*, 1400–1458. [CrossRef] [PubMed]
2. Strehlitz, B.; Nikolaus, N.; Stoltenburg, R. Protein Detection with Aptamer Biosensors. *Sensors* **2008**, *8*, 4296–4307. [CrossRef] [PubMed]
3. Smutok, O.; Katz, E. Biosensors: Electrochemical Devices-General Concepts and Performance. *Biosensors* **2022**, *13*, 44. [CrossRef] [PubMed]
4. Belluzo, M.; Ribone, M.; Lagier, C. Assembling Amperometric Biosensors for Clinical Diagnostics. *Sensors* **2008**, *8*, 1366–1399. [CrossRef]
5. Lin, J.; Chen, Y.; Liu, X.; Jiang, H.; Wang, X. Engineered Intelligent Electrochemical Biosensors for Portable Point-of-Care Diagnostics. *Chemosensors* **2025**, *13*, 146. [CrossRef]
6. Kuswandi, B.; Amalia, R.; Pitaloka, D.A.E.; Murti, B.T.; Hidayat, M.A. Electrochemical nanobiosensors for low-cost clinical diagnosis. *Int. J. Electrochem. Sci.* **2025**, *20*, 101205. [CrossRef]

7. Zhu, C.; Yang, G.; Li, H.; Du, D.; Lin, Y. Electrochemical sensors and biosensors based on nanomaterials and nanostructures. *Anal. Chem.* **2015**, *87*, 230–249. [CrossRef]
8. Pour, S.R.S.; Calabria, D.; Emamiamin, A.; Lazzarini, E.; Pace, A.; Guardigli, M.; Zangheri, M.; Mirasoli, M. Electrochemical vs. Optical Biosensors for Point-of-Care Applications: A Critical Review. *Chemosensors* **2023**, *11*, 546. [CrossRef]
9. Parihar, M.; Niharika, W.N.; Sahana; Biswas, R.; Dehury, B.; Mazumder, N. Point-of-care biosensors for infectious disease diagnosis: Recent updates and prospects. *RSC Adv.* **2025**, *15*, 29267–29283. [CrossRef]
10. Pohanka, M. Aptamers in Electrochemical Biosensors. *Int. J. Electrochem. Sci.* **2022**, *17*, 220659. [CrossRef]
11. Song, S.; Wang, L.; Li, J.; Fan, C.; Zhao, J. Aptamer-based biosensors. *TrAC Trends Anal. Chem.* **2008**, *27*, 108–117. [CrossRef]
12. Yang, L.F.; Ling, M.; Kacherovsky, N.; Pun, S.H. Aptamers 101: Aptamer discovery and in vitro applications in biosensors and separations. *Chem. Sci.* **2023**, *14*, 4961–4978. [CrossRef]
13. Crivianu-Gaita, V.; Thompson, M. Aptamers, antibody scFv, and antibody Fab' fragments: An overview and comparison of three of the most versatile biosensor biorecognition elements. *Biosens. Bioelectron.* **2016**, *85*, 32–45. [CrossRef]
14. Sun, G.; Wei, X.; Zhang, D.; Huang, L.; Liu, H.; Fang, H. Immobilization of Enzyme Electrochemical Biosensors and Their Application to Food Bioprocess Monitoring. *Biosensors* **2023**, *13*, 886. [CrossRef]
15. Zhuo, Z.; Yu, Y.; Wang, M.; Li, J.; Zhang, Z.; Liu, J.; Wu, X.; Lu, A.; Zhang, G.; Zhang, B. Recent Advances in SELEX Technology and Aptamer Applications in Biomedicine. *Int. J. Mol. Sci.* **2017**, *18*, 2142. [CrossRef] [PubMed]
16. Lam, S.Y.; Lau, H.L.; Kwok, C.K. Capture-SELEX: Selection Strategy, Aptamer Identification, and Biosensing Application. *Biosensors* **2022**, *12*, 1142. [CrossRef] [PubMed]
17. Lee, J.O.; So, H.M.; Jeon, E.K.; Chang, H.; Won, K.; Kim, Y.H. Aptamers as molecular recognition elements for electrical nanobiosensors. *Anal. Bioanal. Chem.* **2008**, *390*, 1023–1032. [CrossRef] [PubMed]
18. Abe, K.; Yoshida, W.; Ikebukuro, K. Electrochemical biosensors using aptamers for theranostics. *Adv. Biochem. Eng. Biotechnol.* **2014**, *140*, 183–202. [CrossRef] [PubMed]
19. Zhou, L.; Wang, M.-H.; Wang, J.-P.; Ye, Z.-Z. Application of Biosensor Surface Immobilization Methods for Aptamer. *Chin. J. Anal. Chem.* **2011**, *39*, 432–438. [CrossRef]
20. Sun, H.; Wang, N.; Zhang, L.; Meng, H.; Li, Z. Aptamer-Based Sensors for Thrombin Detection Application. *Chemosensors* **2022**, *10*, 255. [CrossRef]
21. Eissa, S.; Zourob, M. Aptamer- Based Label-Free Electrochemical Biosensor Array for the Detection of Total and Glycated Hemoglobin in Human Whole Blood. *Sci. Rep.* **2017**, *7*, 1016. [CrossRef]
22. Han, K.; Liang, Z.; Zhou, N. Design Strategies for Aptamer-Based Biosensors. *Sensors* **2010**, *10*, 4541–4557. [CrossRef]
23. Saputra, H.A. Electrochemical sensors: Basic principles, engineering, and state of the art. *Monatshefte Für Chem. Chem. Mon.* **2023**, *154*, 1083–1100. [CrossRef]
24. Radi, A.-E.; Abd-Ellatief, M.R. Electrochemical Aptasensors: Current Status and Future Perspectives. *Diagnostics* **2021**, *11*, 104. [CrossRef] [PubMed]
25. Dauphin-Ducharme, P.; Churcher, Z.R.; Shoara, A.A.; Rahbarimehr, E.; Slavkovic, S.; Fontaine, N.; Boisvert, O.; Johnson, P.E. Redox Reporter—Ligand Competition to Support Signaling in the Cocaine-Binding Electrochemical Aptamer-Based Biosensor. *Chemistry* **2023**, *29*, e202300618. [CrossRef] [PubMed]
26. Bao, W.; Aodeng, G.; Ga, L.; Ai, J. Aptamer-based electrochemical biosensors: Signal transduction mechanisms, application progress, and future trends. *Sens. Actuators Rep.* **2025**, *10*, 100366. [CrossRef]
27. Mello, G.A.B.; Benjamin, S.R.; de Lima, F.; Dutra, R.F. Recent Advances in Electrochemical Sensors for the Detection of Anti-Inflammatory and Antibiotic Drugs: A Comprehensive Review. *Biosensors* **2025**, *15*, 676. [CrossRef]
28. Verrinder, E.; Leung, K.K.; Erdal, M.K.; Sepunaru, L.; Plaxco, K.W. Comparison of voltammetric methods used in the interrogation of electrochemical aptamer-based sensors. *Sens. Diagn.* **2024**, *3*, 95–103. [CrossRef]
29. Zhang, H.; Sun, Z.; Sun, K.; Liu, Q.; Chu, W.; Fu, L.; Dai, D.; Liang, Z.; Lin, C.T. Electrochemical Impedance Spectroscopy-Based Biosensors for Label-Free Detection of Pathogens. *Biosensors* **2025**, *15*, 443. [CrossRef]
30. Li, F.; Yu, Z.; Han, X.; Lai, R.Y. Electrochemical aptamer-based sensors for food and water analysis: A review. *Anal. Chim. Acta* **2019**, *1051*, 1–23. [CrossRef]
31. Aller Pellitero, M.; de-los-Santos-Álvarez, N.; Lobo-Castañón, M.J. Aptamer-based electrochemical approaches to meet some of the challenges in the fight against cancer. *Curr. Opin. Electrochem.* **2023**, *39*, 101286. [CrossRef]
32. Mo, T.; Liu, X.; Luo, Y.; Zhong, L.; Zhang, Z.; Li, T.; Gan, L.; Liu, X.; Li, L.; Wang, H.; et al. Aptamer-based biosensors and application in tumor theranostics. *Cancer Sci.* **2021**, *113*, 7–16. [CrossRef]
33. Sikaroodi, M.; Galachiantz, Y.; Baranova, A. Tumor markers: The potential of "omics" approach. *Curr. Mol. Med.* **2010**, *10*, 249–257. [CrossRef] [PubMed]
34. Sadighbayan, D.; Sadighbayan, K.; Tohid-kia, M.R.; Khosroushahi, A.Y.; Hasanzadeh, M. Development of electrochemical biosensors for tumor marker determination towards cancer diagnosis: Recent progress. *TrAC Trends Anal. Chem.* **2019**, *118*, 73–88. [CrossRef]

35. Zhou, H.; Du, X.; Zhang, Z. Electrochemical Sensors for Detection of Markers on Tumor Cells. *Int. J. Mol. Sci.* **2021**, *22*, 8184. [CrossRef]
36. Kam, N.-W.; Laczka, O.; Li, X.; Wilkinson, J.; Hung, D.; Lai, S.P.H.; Wu, K.C.; Tsao, S.W.; Dai, W.; Che, C.M.; et al. ENOX2 inhibition enhances infiltration of effector memory T-cell and mediates response to chemotherapy in immune-quiescent nasopharyngeal carcinoma. *J. Adv. Res.* **2024**, *56*, 69–86. [CrossRef]
37. Böcker, M.; Chatziioannou, E.; Niessner, H.; Hirn, C.; Busch, C.; Ikenberg, K.; Kalbacher, H.; Handgretinger, R.; Sinnberg, T. Ecto-NOX Disulfide-Thiol Exchanger 2 (ENOX2/tNOX) Is a Potential Prognostic Marker in Primary Malignant Melanoma and May Serve as a Therapeutic Target. *Int. J. Mol. Sci.* **2024**, *25*, 11853. [CrossRef]
38. Quansah, M.; Bonham, A.J. Development of an Electrochemical, DNA-Based Biosensor to the Cancer Biomarker ENOX2. *FASEB J.* **2022**, *36*, R3634. [CrossRef]
39. Quansah, M.; Fetter, L.; Fineran, A.; Colling, H.V.; Silver, K.; Rowland, T.J.; Bonham, A.J. Rapid and Quantitative Detection of Lung Cancer Biomarker ENOX2 Using a Novel Aptamer in an Electrochemical DNA-Based (E-DNA) Biosensor. *Biosensors* **2023**, *13*, 675. [CrossRef]
40. Williams, S.C.P. Circulating tumor cells. *Proc. Natl. Acad. Sci. USA* **2013**, *110*, 4861. [CrossRef]
41. Wang, L.; Li, Y.; Xu, J.; Zhang, A.; Wang, X.; Tang, R.; Zhang, X.; Yin, H.; Liu, M.; Wang, D.D.; et al. Quantified postsurgical small cell size CTCs and EpCAM+ circulating tumor stem cells with cytogenetic abnormalities in hepatocellular carcinoma patients determine cancer relapse. *Cancer Lett.* **2018**, *412*, 99–107. [CrossRef]
42. Miao, P.; Tang, Y. Gold Nanoparticles-Based Multipedal DNA Walker for Ratiometric Detection of Circulating Tumor Cell. *Anal. Chem.* **2019**, *91*, 15187–15192. [CrossRef] [PubMed]
43. Peng, Y.; Lu, B.; Deng, Y.; Yang, N.; Li, G. A dual-recognition-controlled electrochemical biosensor for accurate and sensitive detection of specific circulating tumor cells. *Biosens. Bioelectron.* **2022**, *201*, 113973. [CrossRef] [PubMed]
44. Liu, D.; Tang, J.; Xu, H.; Yuan, K.; Aryee, A.A.; Zhang, C.; Meng, H.; Qu, L.; Li, Z. Split-aptamer mediated regenerable temperature-sensitive electrochemical biosensor for the detection of tumour exosomes. *Anal. Chim. Acta* **2022**, *1219*, 340027. [CrossRef] [PubMed]
45. Wang, X.; Huang, J.; Chen, W.; Li, G.; Li, Z.; Lei, J. The updated role of exosomal proteins in the diagnosis, prognosis, and treatment of cancer. *Exp. Mol. Med.* **2022**, *54*, 1390–1400. [CrossRef]
46. Li, D.; Lai, W.; Fan, D.; Fang, Q. Protein biomarkers in breast cancer-derived extracellular vesicles for use in liquid biopsies. *Am. J. Physiol. Cell Physiol.* **2021**, *321*, C779–C797. [CrossRef]
47. Cao, Y.; Yu, X.; Zeng, T.; Fu, Z.; Zhao, Y.; Nie, B.; Zhao, J.; Yin, Y.; Li, G. Molecular Characterization of Exosomes for Subtype-Based Diagnosis of Breast Cancer. *J. Am. Chem. Soc.* **2022**, *144*, 13475–13486. [CrossRef]
48. Cheng, W.; Yao, Y.; Li, D.; Duan, C.; Wang, Z.; Xiang, Y. Asymmetrically split DNAzyme-based colorimetric and electrochemical dual-modal biosensor for detection of breast cancer exosomal surface proteins. *Biosens. Bioelectron.* **2023**, *238*, 115552. [CrossRef]
49. Li, N.; Zhang, Y.; Xu, Y.; Liu, X.; Ma, W.; Xiang, T.; Hou, C.; Huo, D. An ultrasensitive label-free fluorescent aptamer sensor based on pH-gated release coumarin for detect HER2. *Spectrochim. Acta Part A Mol. Biomol. Spectrosc.* **2023**, *296*, 122641. [CrossRef]
50. Singh, G.; Al-Fahad, D.; Al-Zrkani, M.K.; Chaudhuri, T.K.; Soni, H.; Tandon, S.; Narasimhaji, C.V.; Azam, F.; Patil, R. Identification of potential inhibitors of HER2 targeting breast cancer—A structure-based drug design approach. *J. Biomol. Struct. Dyn.* **2023**, *42*, 8184–8201. [CrossRef]
51. Ferreira, D.C.; Batistuti, M.R.; Bachour, B.; Mulato, M. Aptasensor based on screen-printed electrode for breast cancer detection in undiluted human serum. *Bioelectrochemistry* **2021**, *137*, 107586. [CrossRef]
52. Crulhas, B.P.; Karpik, A.E.; Delella, F.K.; Castro, G.R.; Pedrosa, V.A. Electrochemical aptamer-based biosensor developed to monitor PSA and VEGF released by prostate cancer cells. *Anal. Bioanal. Chem.* **2017**, *409*, 6771–6780. [CrossRef]
53. Yan, R.; Lu, N.; Han, S.; Lu, Z.; Xiao, Y.; Zhao, Z.; Zhang, M. Simultaneous detection of dual biomarkers using hierarchical MoS_2 nanostructuring and nano-signal amplification-based electrochemical aptasensor toward accurate diagnosis of prostate cancer. *Biosens. Bioelectron.* **2022**, *197*, 113797. [CrossRef] [PubMed]
54. Huang, P.; Wang, B.; Xing, Y.; Wu, Z.; Li, B.; Liu, L. Detection with Active Capture of Breast Cancer Marker MUC1 Using a MXene-Based Electrochemical Actuator. *ACS Appl. Mater. Interfaces* **2025**, *17*, 33606–33617. [CrossRef] [PubMed]
55. Chandio, I.; Cheung, S.; Ai, Y.; Liang, Q. High-entropy alloy nanoparticles integrated with metal-organic framework for enhanced aptasensing of carcinoembryonic antigen. *Microchem. J.* **2025**, *209*, 112760. [CrossRef]
56. He, K.; Wang, H.; Luo, T.; Yan, F.; Guo, J. Amino-functionalized vertically ordered mesoporous silica film on electrochemically polarized screen-printed carbon electrodes for the construction of gated electrochemical aptasensors and sensitive detection of carcinoembryonic antigens. *Front. Chem.* **2024**, *12*, 1490940. [CrossRef]
57. Kirlangiç, I.A.; Üner, G.; Kara, P.; Kirmizibayrak, P.B.; Ertaş, F.N. Development of transition metal oxide platforms for aptasensing of PSA in cell cultures. *Anal. Bioanal. Chem.* **2024**, *416*, 6421–6435. [CrossRef]
58. Rana, M.S.; Meng, F.; Zhang, R.; Huang, L.; Qian, K. Integrating zirconia-gold hybrid into aptasensor capable of ultrasensitive and robust carcinoembryonic antigen determination. *Electrochim. Acta* **2024**, *507*, 145063. [CrossRef]

59. Rawat, R.; Roy, S.; Goswami, T.; Mirsafi, F.S.; Ismael, M.; Leissner, T.; Mishra, Y.K.; McLaughlin, J.; Kant, K.; Mathur, A. Aptamer-enhanced ultrasensitive electrochemical detection of HER-2 in breast cancer diagnosis using ZnO tetrapod-K4PTC nanohybrids. *Sci. Rep.* **2025**, *15*, 17173. [CrossRef]
60. Ma, H.; Li, J.; Gao, M.; Dong, Y.; Luo, Y.; Su, S. An Electrochemical Aptasensor for Accurate and Sensitive Detection of Exosomes Based on Dual-Probe Recognition and Hybridization Chain Reaction. *Biosensors* **2025**, *15*, 302. [CrossRef]
61. Ma, Y.; Wu, M.; Mo, F.; Chen, Z.; Lu, J.; Sun, D. Enhanced Electrochemical Characterization of the Immune Checkpoint Protein PD-L1 using Aptamer-Functionalized Magnetic Metal-Organic Frameworks. *Adv. Healthc. Mater.* **2024**, *13*, 2303103. [CrossRef]
62. Wang, Y.; Jie, H.; Ye, H.; Zhang, Y.; Li, N.; Zhuang, J. Methylene Blue-Stained Single-Stranded DNA Aptamers as a Highly Efficient Electronic Switch for Quasi-Reagentless Exosomes Detection: An Old Dog with New Tricks. *Anal. Chem.* **2023**, *95*, 18166–18173. [CrossRef]
63. Farokhi, S.; Roushani, M.; Saedi, Z. Fabrication of an electrochemical aptasensor for the determination of sarcosine based on synthesized $CuCo_2O_4$ nanosheets. *Anal. Methods* **2023**, *15*, 4938–4945. [CrossRef] [PubMed]
64. Phetsang, S.; Jouanne, C.; Mallouki, M.; Pham-Truong, T.-N.; Peralta, S.; Vancaeyzeele, C.; Banet, P.; Aubert, P.-H.; Jakmunee, J.; Ounnunkad, K. Competitive electrochemical assay of CA19-9 on gold nanoparticles/porous carbons nanohybrid amplified by polyoxometalate/aptamer/graphene quantum dot-decorated gold nanotags. *J. Mater. Chem. B* **2025**, *13*, 11652–11662. [CrossRef] [PubMed]
65. Hatami, Z.; Shamsipur, M.; Jalali, F.; Farzin, L.; Barati, A. A novel antibody-aptamer sandwich-type electrochemical biosensor for femtomolar detection of VEGF165 in patients with lymphoma cancer. *J. Chin. Chem. Soc.* **2025**, *72*, 892–901. [CrossRef]
66. Shang, Z.; Su, T.; Jin, D.; Xu, Q.; Hu, X.; Shu, Y. An integrated and flexible PDMS/Au film-based electrochemical immunosensor via Fe–Co MOF as a signal amplifier for alpha fetoprotein detection. *Biosens. Bioelectron.* **2023**, *230*, 115245. [CrossRef]
67. Cui, C.B.; Yang, G.C.; Zhang, Z.; Wang, X.J. Synthesis of MoS_2/Fe_3O_4 composites for the detection of liver cancer biomarker alpha-fetoprotein. *Chalcogenide Lett.* **2025**, *22*, 507–520. [CrossRef]
68. Xu, Z.; Ouyang, H.; Zhao, S.; Wang, X.; Huo, X.; He, D.; Liu, R. Electroactive Fe_3O_4/α-Fe_2O_3@Au nanocomposites driven label-free electrochemical aptasensor with magnetic self-assembly for rapid quantification of alpha-fetoprotein. *Microchim. Acta* **2025**, *192*, 361. [CrossRef]
69. Chen, X.F.; Zhao, X.; Yang, Z. Aptasensors for the detection of infectious pathogens: Design strategies and point-of-care testing. *Microchim. Acta* **2022**, *189*, 443. [CrossRef]
70. Sunnetcioglu, A.; Sunnetcioglu, M.; Binici, I.; Baran, A.I.; Karahocagil, M.K.; Saydan, M.R. Comparative analysis of pulmonary and extrapulmonary tuberculosis of 411 cases. *Ann. Clin. Microbiol. Antimicrob.* **2015**, *14*, 34. [CrossRef]
71. Ramalingam, G.; Jayaraman, S.; Khan, J.M.; Ahmed, M.Z.; Ahmad, A.; Manickan, E.; Rajagopal, P. Exploring recombinant secretory proteins from *Mycobacterium tuberculosis* to develop a serological platform for tuberculosis diagnosis. *Int. J. Biol. Macromol.* **2023**, *249*, 126769. [CrossRef] [PubMed]
72. MacLean, E.; Kohli, M.; Weber, S.F.; Suresh, A.; Schumacher, S.G.; Denkinger, C.M.; Pai, M. Advances in Molecular Diagnosis of Tuberculosis. *J. Clin. Microbiol.* **2020**, *58*, e01582-19. [CrossRef] [PubMed]
73. Huang, H.; Chen, Y.; Zuo, J.; Deng, C.; Fan, J.; Bai, L.; Guo, S. MXene-incorporated C_{60}NPs and Au@Pt with dual-electric signal outputs for accurate detection of *Mycobacterium tuberculosis* ESAT-6 antigen. *Biosens. Bioelectron.* **2023**, *242*, 115734. [CrossRef] [PubMed]
74. Asare, K.K.; Azumah, D.E.; Adu-Gyamfi, C.O.; Opoku, Y.K.; Adela, E.M.; Afful, P.; Abotsi, G.K.; Abban, E.A.; Duntu, P.E.; Anyamful, A.; et al. Comparison of microscopic and xpert MTB diagnoses of presumptive mycobacteria tuberculosis infection: Retrospective analysis of routine diagnosis at Cape Coast Teaching Hospital. *BMC Infect. Dis.* **2024**, *24*, 660. [CrossRef]
75. Lee, H.J.; Kim, N.H.; Lee, E.H.; Yoon, Y.S.; Jeong, Y.J.; Lee, B.C.; Koo, B.; Jang, Y.O.; Kim, S.H.; Kang, Y.A.; et al. Multicenter Testing of a Simple Molecular Diagnostic System for the Diagnosis of *Mycobacterium Tuberculosis*. *Biosensors* **2023**, *13*, 259. [CrossRef]
76. Suzuki, H.; Nishizawa, T.; Hibi, T. *Helicobacter pylori* eradication therapy. *Future Microbiol.* **2010**, *5*, 639–648. [CrossRef]
77. Park, J.B.; Koo, J.S. *Helicobacter pylori* infection in gastric mucosa-associated lymphoid tissue lymphoma. *World J. Gastroenterol.* **2014**, *20*, 2751–2759. [CrossRef]
78. Falkeis-Veits, C.; Vieth, M. Non-malignant *Helicobacter pylori*—Associated Diseases. *Adv. Exp. Med. Biol.* **2019**, *1149*, 121–134. [CrossRef]
79. Roushani, M.; Sarabaegi, M.; Hosseini, H.; Pourahmad, F. Gold nanostructures integrated on hollow carbon N-doped nanocapsules as a novel high-performance aptasensing platform for *Helicobacter pylori* detection. *J. Mater. Sci.* **2022**, *57*, 589–597. [CrossRef]
80. Mujtaba, A.; Ibrahim, M.S.; Parveen, S.; Sarwar, N.; Alsagaby, S.A.; Raza, M.A.; Abdelgawad, M.A.; Ghoneim, M.M.; El-Ghorab, A.H.; Selim, S.; et al. Comparative Analysis of Diagnostic Techniques for *Helicobacter pylori* Infection: Insights for Effective Therapy. *J. Cell. Mol. Med.* **2025**, *29*, e70487. [CrossRef]
81. Mi, X.; Li, H.; Tan, R.; Tu, Y. Dual-Modular Aptasensor for Detection of Cardiac Troponin I Based on Mesoporous Silica Films by Electrochemiluminescence/Electrochemical Impedance Spectroscopy. *Anal. Chem.* **2020**, *92*, 14640–14647. [CrossRef]

82. Chen, K.; Zhao, H.; Wang, Z.; Zhou, F.; Shi, Z.; Cao, S.; Lan, M. Sandwich-type electrochemical aptasensor based on Au-modified conductive octahedral carbon architecture and snowflake-like PtCuNi for the sensitive detection of cardiac troponin I. *Biosens. Bioelectron.* **2022**, *212*, 114431. [CrossRef] [PubMed]
83. Zhu, Y.; Sun, S.; Yin, X.; Liu, Y.; Yang, W.; Chen, Y. Carbon Nanotube-Gold Nanoparticle-Based Self-Powered Electrochemical Biosensors for Highly Sensitive and Stable Detection of Myoglobin. *ACS Appl. Nano Mater.* **2023**, *6*, 11085–11094. [CrossRef]
84. Rafe, T.; Shawon, P.A.; Salem, L.; Chowdhury, N.I.; Kabir, F.; Bin Zahur, S.M.; Akhter, R.; Noor, H.B.; Mohib, M.M.; Sagor, M.A.T. Preventive Role of Resveratrol Against Inflammatory Cytokines and Related Diseases. *Curr. Pharm. Des.* **2019**, *25*, 1345–1371. [CrossRef] [PubMed]
85. Bonavita, E.; Gentile, S.; Rubino, M.; Maina, V.; Papait, R.; Kunderfranco, P.; Greco, C.; Feruglio, F.; Molgora, M.; Laface, I.; et al. PTX3 Is an Extrinsic Oncosuppressor Regulating Complement-Dependent Inflammation in Cancer. *Cell* **2015**, *160*, 700–714. [CrossRef]
86. Zhang, H.; Zhou, X.-D.; Shapiro, M.D.; Lip, G.Y.H.; Tilg, H.; Valenti, L.; Somers, V.K.; Byrne, C.D.; Targher, G.; Yang, W.; et al. Global burden of metabolic diseases, 1990–2021. *Metabolism* **2024**, *160*, 155999. [CrossRef]
87. Chen, Y.; Pui, T.S.; Kongsuphol, P.; Tang, K.C.; Arya, S.K. Aptamer-based array electrodes for quantitative interferon-γ detection. *Biosens. Bioelectron.* **2014**, *53*, 257–262. [CrossRef]
88. Qiao, L.; Benzigar, M.R.; Subramony, J.A.; Lovell, N.H.; Liu, G. Advances in Sweat Wearables: Sample Extraction, Real-Time Biosensing, and Flexible Platforms. *ACS Appl. Mater. Interfaces* **2020**, *12*, 34337–34361. [CrossRef]
89. Chu, H.; Hu, X.; Lee, C.-Y.; Zhang, A.; Ye, Y.; Wang, Y.; Chen, Y.; Yan, X.; Wang, X.; Wei, J.; et al. A wearable electrochemical fabric for cytokine monitoring. *Biosens. Bioelectron.* **2023**, *232*, 115301. [CrossRef]
90. Fajgenbaum, D.C.; June, C.H. Cytokine Storm. *N. Engl. J. Med.* **2020**, *383*, 2255–2273. [CrossRef]
91. Shimabukuro-Vornhagen, A.; Gödel, P.; Subklewe, M.; Stemmler, H.J.; Schlößer, H.A.; Schlaak, M.; Kochanek, M.; Böll, B.; von Bergwelt-Baildon, M.S. Cytokine release syndrome. *J. Immunother. Cancer* **2018**, *6*, 56. [CrossRef] [PubMed]
92. Noh, S.; Lee, H.; Kim, J.; Jang, H.; An, J.; Park, C.; Lee, M.-H.; Lee, T. Rapid electrochemical dual-target biosensor composed of an Aptamer/MXene hybrid on Au microgap electrodes for cytokines detection. *Biosens. Bioelectron.* **2022**, *207*, 114159. [CrossRef] [PubMed]
93. Wang, Z.; Hao, Z.; Wang, X.; Huang, C.; Lin, Q.; Zhao, X.; Pan, Y. A Flexible and Regenerative Aptameric Graphene–Nafion Biosensor for Cytokine Storm Biomarker Monitoring in Undiluted Biofluids toward Wearable Applications. *Adv. Funct. Mater.* **2021**, *31*, 2005958. [CrossRef]
94. Boolani, A.; Channaveerappa, D.; Dupree, E.J.; Jayathirtha, M.; Aslebagh, R.; Grobe, S.; Wilkinson, T.; Darie, C.C. Trends in Analysis of Cortisol and Its Derivatives. *Adv. Exp. Med. Biol.* **2019**, *1140*, 649–664. [CrossRef]
95. Ousova, O.; Guyonnet-Duperat, V.; Iannuccelli, N.; Bidanel, J.-P.; Milan, D.; Genêt, C.; Llamas, B.; Yerle, M.; Gellin, J.; Chardon, P.; et al. Corticosteroid Binding Globulin: A New Target for Cortisol-Driven Obesity. *Mol. Endocrinol.* **2004**, *18*, 1687–1696. [CrossRef]
96. Karuppaiah, G.; Velayutham, J.; Hansda, S.; Narayana, N.; Bhansali, S.; Manickam, P. Towards the development of reagent-free and reusable electrochemical aptamer-based cortisol sensor. *Bioelectrochemistry* **2022**, *145*, 108098. [CrossRef]
97. Rahmati, Z.; Roushani, M.; Hosseini, H. MOF-Derived Ni-P Bundle-Like Nanorods as High-Performance Substrate for Design of Electrochemical Aptasensor Toward Cortisol Detection. *IEEE Sens. J.* **2023**, *23*, 1770–1777. [CrossRef]
98. Pantalone, K.M.; Hatipoglu, B.; Gupta, M.K.; Kennedy, L.; Hamrahian, A.H. Measurement of Serum Free Thyroxine Index May Provide Additional Case Detection Compared to Free Thyroxine in the Diagnosis of Central Hypothyroidism. *Case Rep. Endocrinol.* **2015**, *2015*, 965191. [CrossRef]
99. Kashefi-Kheyrabadi, L.; Koyappayil, A.; Kim, T.; Cheon, Y.-P.; Lee, M.-H. A MoS_2@Ti_3C_2Tx MXene hybrid-based electrochemical aptasensor (MEA) for sensitive and rapid detection of Thyroxine. *Bioelectrochemistry* **2021**, *137*, 107674. [CrossRef]
100. Tanoue, R.; Kume, I.; Yamamoto, Y.; Takaguchi, K.; Nomiyama, K.; Tanabe, S.; Kunisue, T. Determination of free thyroid hormones in animal serum/plasma using ultrafiltration in combination with ultra-fast liquid chromatography-tandem mass spectrometry. *J. Chromatogr. A* **2018**, *1539*, 30–40. [CrossRef]
101. Ruuskanen, S.; Hsu, B.-Y.; Heinonen, A.; Vainio, M.; Darras, V.M.; Sarraude, T.; Rokka, A. A new method for measuring thyroid hormones using nano-LC-MS/MS. *J. Chromatogr. B* **2018**, *1093–1094*, 24–30. [CrossRef]
102. Park, S.Y.; Kim, J.; Yim, G.; Jang, H.; Lee, Y.; Kim, S.M.; Park, C.; Lee, M.-H.; Lee, T. Fabrication of electrochemical biosensor composed of multi-functional DNA/rhodium nanoplate heterolayer for thyroxine detection in clinical sample. *Colloids Surf. B Biointerfaces* **2020**, *195*, 111240. [CrossRef] [PubMed]
103. Lu, D.; Cai, R.; Liao, Y.; You, R.; Lu, Y. Two-dimensional glass/p-ATP/Ag NPs as multifunctional SERS substrates for label-free quantification of uric acid in sweat. *Spectrochim. Acta Part A Mol. Biomol. Spectrosc.* **2023**, *296*, 122631. [CrossRef] [PubMed]
104. Yang, S.; Liu, H.; Fang, X.-M.; Yan, F.; Zhang, Y. Signaling pathways in uric acid homeostasis and gout: From pathogenesis to therapeutic interventions. *Int. Immunopharmacol.* **2024**, *132*, 111932. [CrossRef] [PubMed]

105. Ghanbari, M.H.; Mashhadizadeh, M.H.; Norouzi, Z.; Salehzadeh, H. Simultaneous electrochemical detection of uric acid and xanthine based on electrodeposited B, N co-doped reduced graphene oxide, gold nanoparticles and electropolymerized poly (L-cysteine) gradually modified electrode platform. *Microchem. J.* **2022**, *175*, 107213. [CrossRef]
106. Tri Murti, B.; Huang, Y.-J.; Darumas Putri, A.; Lee, C.-P.; Hsieh, C.-M.; Wei, S.-M.; Tsai, M.-L.; Peng, C.-W.; Yang, P.-K. Free-standing vertically aligned tin disulfide nanosheets for ultrasensitive aptasensor design toward Alzheimer's diagnosis applications. *Chem. Eng. J.* **2023**, *452*, 139394. [CrossRef]
107. Liao, X.; Ge, K.; Cai, Z.; Qiu, S.; Wu, S.; Li, Q.; Liu, Z.; Gao, F.; Tang, Q. Hybridization chain reaction triggered poly adenine to absorb silver nanoparticles for label-free electrochemical detection of Alzheimer's disease biomarkers amyloid β-peptide oligomers. *Anal. Chim. Acta* **2022**, *1192*, 339391. [CrossRef]
108. Rahmati, Z.; Roushani, M.; Hosseini, H. Three-dimensional NiCo2O4 nanowires encapsulated in nitrogen-doped carbon networks as a high-performance aptamer stabilizer for impedimetric ultrasensitive detection of hepatitis C virus core antigen. *Surf. Interfaces* **2021**, *22*, 100813. [CrossRef]
109. Lo, Y.; Cheung, Y.-W.; Wang, L.; Lee, M.; Figueroa-Miranda, G.; Liang, S.; Mayer, D.; Tanner, J.A. An electrochemical aptamer-based biosensor targeting *Plasmodium falciparum* histidine-rich protein II for malaria diagnosis. *Biosens. Bioelectron.* **2021**, *192*, 113472. [CrossRef]
110. Gogola, J.L.; Martins, G.; Gevaerd, A.; Blanes, L.; Cardoso, J.; Marchini, F.K.; Banks, C.E.; Bergamini, M.F.; Marcolino-Junior, L.H. Label-free aptasensor for p24-HIV protein detection based on graphene quantum dots as an electrochemical signal amplifier. *Anal. Chim. Acta* **2021**, *1166*, 338548. [CrossRef]
111. Naseri, M.; Halder, A.; Mohammadniaei, M.; Prado, M.; Ashley, J.; Sun, Y. A multivalent aptamer-based electrochemical biosensor for biomarker detection in urinary tract infection. *Electrochim. Acta* **2021**, *389*, 138644. [CrossRef]
112. Gobalu, K.; Vasudevan, M.; Gopinath, S.C.B.; Perumal, V.; Ovinis, M. Molybdenum disulphide/cellulose acetate nanofiber composite on screen printed electrodes for detecting cardiac troponin by electrical impedance spectroscopy. *Cellulose* **2021**, *28*, 5761–5774. [CrossRef]
113. Ma, J.; Feng, L.; Li, J.; Zhu, D.; Wang, L.; Su, S. Biological Recognition-Based Electrochemical Aptasensor for Point-of-Care Detection of cTnI. *Biosensors* **2023**, *13*, 746. [CrossRef]
114. Song, Z.; Song, J.; Gao, F.; Chen, X.; Wang, Q.; Zhao, Y.; Huang, X.; Yang, C.; Wang, Q. Novel electroactive ferrocene-based covalent organic frameworks towards electrochemical label-free aptasensors for the detection of Cardiac Troponin I. *Sens. Actuators B Chem.* **2022**, *368*, 132205. [CrossRef]
115. Yeh, Y.-S.; Yen, Y.-K.; Shanmugam, R. Tungsten disulfide nanotubes enhanced nanocomposite paper-based aptasensor for label-free electrochemical detection of interferon-gamma. *Microchem. J.* **2023**, *193*, 109081. [CrossRef]
116. Azmi, U.Z.M.; Yusof, N.A.; Abdullah, J.; Mohammad, F.; Ahmad, S.A.A.; Suraiya, S.; Raston, N.H.A.; Faudzi, F.N.M.; Khiste, S.K.; Al-Lohedan, H.A. Aptasensor for the Detection of *Mycobacterium tuberculosis* in Sputum Utilising CFP10-ESAT6 Protein as a Selective Biomarker. *Nanomaterials* **2021**, *11*, 2446. [CrossRef] [PubMed]
117. Khan, R.; Deshpande, A.S.; Proteasa, G.; Andreescu, S. Aptamer-based electrochemical biosensor with S protein binding affinity for COVID-19 detection: Integrating computational design with experimental validation of S protein binding affinity. *Sens. Actuators B Chem.* **2024**, *399*, 134775. [CrossRef]
118. Hu, Z.; Zhu, R.; Figueroa-Miranda, G.; Zhou, L.; Feng, L.; Offenhäusser, A.; Mayer, D. Truncated Electrochemical Aptasensor with Enhanced Antifouling Capability for Highly Sensitive Serotonin Detection. *Biosensors* **2023**, *13*, 881. [CrossRef]
119. Malkawi, A.K.; Jafari, M.; Ohlund, L.; Sleno, L.; Abdel Rahman, A.M.; Siaj, M. A diagnostic electrochemical aptasensor development for sCD80 protein detection in human serum. *Biosens. Bioelectron.* **2023**, *242*, 115696. [CrossRef]
120. Chandio, I.; Jiao, Q.; Li, R.; Ai, Y.; Liang, Q. Dual-Signal Electrochemical Aptasensor Based on High-Entropy Alloy Nanosheets for Calprotectin Detection in Inflammatory Bowel Disease. *ACS Appl. Mater. Interfaces* **2025**, *17*, 38960–38970. [CrossRef]
121. Oranzie, M.; January, J.L.; Sanga, N.A.; Leve, Z.D.; Mini, S.; Cupido, C.; Douman, S.F.; Iwuoha, E.I. Aptamer-Driven Biosensor Technology for the Quantitative Analysis of C-Reactive Protein. *ChemElectroChem* **2025**, *12*, e202400667. [CrossRef]
122. Lafi, Z.; Gharaibeh, L.; Nsairat, H.; Asha, N.; Alshaer, W. Aptasensors: Employing Molecular Probes for Precise Medical Diagnostics and Drug Monitoring. *Bioanalysis* **2023**, *15*, 1439–1460. [CrossRef]
123. Aslan, Y.; Atabay, M.; Chowdhury, H.K.; Göktürk, I.; Saylan, Y.; Inci, F. Aptamer-Based Point-of-Care Devices: Emerging Technologies and Integration of Computational Methods. *Biosensors* **2023**, *13*, 569. [CrossRef] [PubMed]
124. Zhong, S.; Chen, L.; Shi, X.; Chen, G.; Sun, D.; Zhang, L. Recent advances in electrochemical aptasensors for detecting cardiac biomarkers: A review. *Microchem. J.* **2023**, *193*, 109063. [CrossRef]
125. Gabrusenok, P.V.; Ramazanov, R.R.; Kasyanenko, N.A.; Lantushenko, A.O.; Sokolov, P.A. pH-dependent binding of ATP aptamer to the target and competition strands: Fluorescent melting curve fitting study. *Biochim. Biophys. Acta Gen. Subj.* **2024**, *1868*, 130689. [CrossRef] [PubMed]

126. Schmidt, C.; Kammel, A.; Tanner, J.A.; Kinghorn, A.B.; Khan, M.M.; Lehmann, W.; Menger, M.; Schedler, U.; Schierack, P.; Rodiger, S. A multiparametric fluorescence assay for screening aptamer-protein interactions based on microbeads. *Sci. Rep.* **2022**, *12*, 2961. [CrossRef]
127. Chandio, I.; Rahujo, S.; Chandio, Z.A.; Rashid, M.A.; Rehman, M.U.; Shar, Z.H.; Thebo, K.H. Recent development in metal-organic frameworks-based electrochemical aptasensors for detection of cancer biomarkers. *Bioelectrochemistry* **2025**, *165*, 109006. [CrossRef]
128. Omage, J.I.; Easterday, E.; Rumph, J.T.; Brula, I.; Hill, B.; Kristensen, J.; Ha, D.T.; Galindo, C.L.; Danquah, M.K.; Sims, N.; et al. Cancer Diagnostics and Early Detection Using Electrochemical Aptasensors. *Micromachines* **2022**, *13*, 522. [CrossRef]
129. Cho, M.-S.; Kim, Y.-W.; Han, S.-Y.; Min, K.-I.; Rahman, M.A.; Shim, Y.-B.; Ban, C.-I. Detection for folding of the thrombin binding aptamer using label-free electrochemical methods. *BMB Rep.* **2008**, *41*, 126–131. [CrossRef]
130. Pellitero, M.A.; Curtis, S.D.; Arroyo-Curras, N. Interrogation of Electrochemical Aptamer-Based Sensors via Peak-to-Peak Separation in Cyclic Voltammetry Improves the Temporal Stability and Batch-to-Batch Variability in Biological Fluids. *ACS Sens.* **2021**, *6*, 1199–1207. [CrossRef]
131. Tsai, Y.C.; Weng, W.Y.; Yeh, Y.T.; Chien, J.C. Dual-Aptamer Drift Canceling Techniques to Improve Long-Term Stability of Real-Time Structure-Switching Aptasensors. *ACS Sens.* **2023**, *8*, 3380–3388. [CrossRef] [PubMed]
132. Animesh, S.; Singh, Y.D. A Comprehensive Study on Aptasensors for Cancer Diagnosis. *Curr. Pharm. Biotechnol.* **2021**, *22*, 1069–1084. [CrossRef] [PubMed]
133. Velusamy, V.; Arshak, K.; Korostynska, O.; Oliwa, K.; Adley, C. An overview of foodborne pathogen detection: In the perspective of biosensors. *Biotechnol. Adv.* **2010**, *28*, 232–254. [CrossRef] [PubMed]
134. Majdinasab, M.; Daneshi, M.; Louis Marty, J. Recent developments in non-enzymatic (bio)sensors for detection of pesticide residues: Focusing on antibody, aptamer and molecularly imprinted polymer. *Talanta* **2021**, *232*, 122397. [CrossRef]
135. Zhang, Z.; Lou, Y.; Guo, C.; Jia, Q.; Song, Y.; Tian, J.-Y.; Zhang, S.; Wang, M.; He, L.; Du, M. Metal–organic frameworks (MOFs) based chemosensors/biosensors for analysis of food contaminants. *Trends Food Sci. Technol.* **2021**, *118*, 569–588. [CrossRef]
136. Mishra, G.K.; Barfidokht, A.; Tehrani, F.; Mishra, R.K. Food Safety Analysis Using Electrochemical Biosensors. *Foods* **2018**, *7*, 141. [CrossRef]
137. Ricci, F.; Volpe, G.; Micheli, L.; Palleschi, G. A review on novel developments and applications of immunosensors in food analysis. *Anal. Chim. Acta* **2007**, *605*, 111–129. [CrossRef]
138. Lan, L.; Yao, Y.; Ping, J.; Ying, Y. Recent advances in nanomaterial-based biosensors for antibiotics detection. *Biosens. Bioelectron.* **2017**, *91*, 504–514. [CrossRef]
139. Malecka-Baturo, K.; Zaganiaris, A.; Grabowska, I.; Kurzątkowska-Adaszyńska, K. Electrochemical Biosensor Designed to Distinguish Tetracyclines Derivatives by ssDNA Aptamer Labelled with Ferrocene. *Int. J. Mol. Sci.* **2022**, *23*, 13785. [CrossRef]
140. Wei, X.; Sun, Y.; Luo, Y.; Shu, R.; Lin, H.; Xu, D. Electrochemical biosensor Bi2O3@Au@Apta based on Bi2O3 nanofibers for sensitive detection of ampicillin. *Biochem. Eng. J.* **2023**, *200*, 109107. [CrossRef]
141. Bao, Y.; Cai, K.; Liu, Y.; Li, B. Aptamer-Based Antibiotic Electrochemical Detection Platform Using Portable Plastic Gold Electrode and Multichannel Chip. *Chin. J. Chem.* **2024**, *42*, 171–176. [CrossRef]
142. Akbarzadeh, S.; Khajehsharifi, H.; Hajihosseini, S. Detection of Oxytetracycline Using an Electrochemical Label-Free Aptamer-Based Biosensor. *Biosensors* **2022**, *12*, 468. [CrossRef] [PubMed]
143. Alshannaq, A.; Yu, J.-H. Occurrence, Toxicity, and Analysis of Major Mycotoxins in Food. *Int. J. Environ. Res. Public Health* **2017**, *14*, 632. [CrossRef] [PubMed]
144. Boudra, H.; Barnouin, J.; Dragacci, S.; Morgavi, D.P. Aflatoxin M1 and Ochratoxin A in Raw Bulk Milk from French Dairy Herds. *J. Dairy Sci.* **2007**, *90*, 3197–3201. [CrossRef] [PubMed]
145. Kanungo, L.; Pal, S.; Bhand, S. Miniaturised hybrid immunoassay for high sensitivity analysis of aflatoxin M1 in milk. *Biosens. Bioelectron.* **2011**, *26*, 2601–2606. [CrossRef]
146. Yang, D.; Hui, Y.; Liu, Y.; Wang, W.; He, C.; Zhao, A.; Wei, L.; Wang, B. Novel dual-recognition electrochemical biosensor for the sensitive detection of AFM1 in milk. *Food Chem.* **2024**, *433*, 137362. [CrossRef]
147. Guo, L.; Cui, Z.; Xue, J.; Zhang, Y.; Yang, H.; Miao, M. Cascade signal amplification electrochemical biosensor based on AgNPs and ring opening polymerization for determination of Ochratoxin A. *Microchim. Acta* **2023**, *190*, 432. [CrossRef]
148. Bougrini, M.; Baraket, A.; Jamshaid, T.; El Aissari, A.; Bausells, J.; Zabala, M.; El Bari, N.; Bouchikhi, B.; Jaffrezic-Renault, N.; Abdelhamid, E.; et al. Development of a novel capacitance electrochemical biosensor based on silicon nitride for ochratoxin A detection. *Sens. Actuators B Chem.* **2016**, *234*, 446–452. [CrossRef]
149. Karczmarczyk, A.; Baeumner, A.J.; Feller, K.-H. Rapid and sensitive inhibition-based assay for the electrochemical detection of Ochratoxin A and Aflatoxin M1 in red wine and milk. *Electrochim. Acta* **2017**, *243*, 82–89. [CrossRef]
150. Jodra, A.; Hervás, M.; López, M.Á.; Escarpa, A. Disposable electrochemical magneto immunosensor for simultaneous simplified calibration and determination of Ochratoxin A in coffee samples. *Sens. Actuators B Chem.* **2015**, *221*, 777–783. [CrossRef]

151. Wei, C.; Zhong, J.; Hu, T.; Zhao, X. Simultaneous detection of *Escherichia coli* O157:H7, *Staphylococcus aureus* and *Salmonella* by multiplex PCR in milk. *3 Biotech* **2018**, *8*, 76. [CrossRef] [PubMed]
152. Sharma, H.; Agarwal, M.; Goswami, M.; Sharma, A.; Roy, S.K.; Rai, R.; Murugan, M.S. Biosensors: Tool for food borne pathogen detection. *Vet. World* **2013**, *6*, 968–973. [CrossRef]
153. Scallan, E.; Hoekstra, R.M.; Angulo, F.J.; Tauxe, R.V.; Widdowson, M.-A.; Roy, S.L.; Jones, J.L.; Griffin, P.M. Foodborne Illness Acquired in the United States—Major Pathogens. *Emerg. Infect. Dis.* **2011**, *17*, 7–15. [CrossRef] [PubMed]
154. Kirk, M.D.; Pires, S.M.; Black, R.E.; Caipo, M.; Crump, J.A.; Devleesschauwer, B.; Döpfer, D.; Fazil, A.; Fischer-Walker, C.L.; Hald, T.; et al. World Health Organization Estimates of the Global and Regional Disease Burden of 22 Foodborne Bacterial, Protozoal, and Viral Diseases, 2010: A Data Synthesis. *PLoS Med.* **2015**, *12*, e1001940. [CrossRef]
155. Cheung, G.Y.C.; Bae, J.S.; Otto, M. Pathogenicity and virulence of *Staphylococcus aureus*. *Virulence* **2021**, *12*, 547–569. [CrossRef]
156. Zhao, X.; Lin, C.-W.; Wang, J.; Oh, D.H. Advances in Rapid Detection Methods for Foodborne Pathogens. *J. Microbiol. Biotechnol.* **2014**, *24*, 297–312. [CrossRef]
157. Li, N.; Zhang, Y.; Wei, T.; Yang, T.; Bao, Q.; Cheng, Q.; Mao, C.; Shuai, Y.; Yang, M. Upconversion nanoparticle-based aptasensor for rapid and ultrasensitive detection of *Staphylococcus aureus* by low-speed centrifugation. *RSC Adv.* **2023**, *13*, 20229–20234. [CrossRef]
158. Hui, Y.; Peng, H.; Zhang, F.; Zhang, L.; Liu, Y.; Jia, R.; Song, Y.; Wang, B. An ultrasensitive sandwich-type electrochemical aptasensor using silver nanoparticle/titanium carbide nanocomposites for the determination of *Staphylococcus aureus* in milk. *Microchim. Acta* **2022**, *189*, 276. [CrossRef]
159. Nguyen, T.T.-Q.; Kim, E.R.; Gu, M.B. A new cognate aptamer pair-based sandwich-type electrochemical biosensor for sensitive detection of *Staphylococcus aureus*. *Biosens. Bioelectron.* **2022**, *198*, 113835. [CrossRef]
160. Appaturi, J.N.; Pulingam, T.; Thong, K.L.; Muniandy, S.; Ahmad, N.; Leo, B.F. Rapid and sensitive detection of *Salmonella* with reduced graphene oxide-carbon nanotube based electrochemical aptasensor. *Anal. Biochem.* **2020**, *589*, 113489. [CrossRef]
161. Li, Z.; Zhang, X.; Qi, H.; Huang, X.; Shi, J.; Zou, X. A novel renewable electrochemical biosensor based on mussel-inspired adhesive protein for the detection of *Escherichia coli* O157:H7 in food. *Sens. Actuators B Chem.* **2022**, *372*, 132601. [CrossRef]
162. Dabhade, A.H.; Verma, R.P.; Paramasivan, B.; Kumawat, A.; Saha, B. Development of silver nanoparticles and aptamer conjugated biosensor for rapid detection of *E. coli* in a water sample. *3 Biotech* **2023**, *13*, 244. [CrossRef] [PubMed]
163. Tian, J.-Y.; Liu, X.; Zhang, S.; Chen, K.; Zhu, L.; Song, Y.; Wang, M.; Zhang, Z.; Du, M. Novel aptasensing strategy for efficiently quantitative analyzing *Staphylococcus aureus* based on defective copper-based metal–organic framework. *Food Chem.* **2023**, *402*, 134357. [CrossRef] [PubMed]
164. Cai, R.; Zhang, S.; Chen, L.; Li, M.; Zhang, Y.; Zhou, N. Self-Assembled DNA Nanoflowers Triggered by a DNA Walker for Highly Sensitive Electrochemical Detection of *Staphylococcus aureus*. *ACS Appl. Mater. Interfaces* **2021**, *13*, 4905–4914. [CrossRef]
165. Somayeh, S.S.; Taghdisi, S.M.; Mortazavi, S.A.; Farideh, T.Y.; Abnous, K. A novel electrochemical biosensor for detection of micrococcal nuclease in milk based on a U-shaped DNA structure. *Talanta* **2023**, *253*, 123989. [CrossRef]
166. Shan, X.; Xie, H.; Zhou, T.; Wu, M.; Yang, J. Dual DNA recycling amplifications coupled with Au NPs@ZIF-MOF accelerator for enhanced electrochemical ratiometric sensing of pathogenic bacteria. *Talanta* **2023**, *263*, 124751. [CrossRef]
167. Morsalpour, H.; Zare, H.R.; Shekari, Z.; Mirbagheri, M. Development of an electrochemical sensitive aptasensor based on a zeolite imidazolate framework-8 and gold nanoparticles for the determination of *Staphylococcus aureus* bacteria. *Anal. Bioanal. Chem.* **2024**, *416*, 1229–1238. [CrossRef]
168. Jiang, H.; Sun, Z.; Zhang, C.; Weng, X. 3D-architectured aptasensor for ultrasensitive electrochemical detection of norovirus based on phosphorene-gold nanocomposites. *Sens. Actuators B Chem.* **2022**, *354*, 131232. [CrossRef]
169. Zhao, H.; Xie, W.; Zhang, R.-L.; Wang, X.-D.; Liu, H.-F.; Li, J.; Sha, T.; Guo, X.-S.; Li, J.; Sun, Q.-M.; et al. Electrochemical sensor for human norovirus based on covalent organic framework/pillararene heterosupramolecular nanocomposites. *Talanta* **2022**, *237*, 122896. [CrossRef]
170. Wang, W.; Xiao, S.; Jia, Z.; Xie, H.; Li, T.; Wang, Q.; Gan, N. A dual-mode aptasensor for foodborne pathogens detection using Pt, phenylboric acid and ferrocene modified Ti_3C_2 MXenes nanoprobe. *Sens. Actuators B Chem.* **2022**, *351*, 130839. [CrossRef]
171. Mishra, A.; Pilloton, R.; Jain, S.; Roy, S.; Khanuja, M.; Mathur, A.; Narang, J. Paper-Based Electrodes Conjugated with Tungsten Disulfide Nanostructure and Aptamer for Impedimetric Detection of *Listeria monocytogenes*. *Biosensors* **2022**, *12*, 88. [CrossRef]
172. Oliveira, D.A.; McLamore, E.S.; Gomes, C.L. Rapid and label-free *Listeria monocytogenes* detection based on stimuli-responsive alginate-platinum thiomer nanobrushes. *Sci. Rep.* **2022**, *12*, 21413. [CrossRef]
173. Li, Z.; Zhao, L.; Wu, Q.; Zhang, X.; Huang, X.; Shi, J.; Zou, X. A Renewable Biosensor Based on LNA-Aptamer Hybridization for the Detection of *Salmonella enteritidis* in *Penaeus vannamei*. *Molecules* **2023**, *28*, 450. [CrossRef]
174. Khattiya, A.; Karaket, R.; Mathaweesansurn, A.; Detsri, E. Ultrasensitive electrochemical aptasensors based on trimetallic AuPt-Ru nanoparticles decorated RGO with disposable and low-cost goldleaf electrode for aflatoxin B1 quantification in agricultural products. *Microchem. J.* **2025**, *208*, 112631. [CrossRef]

175. Rani, L.; Thapa, K.; Kanojia, N.; Sharma, N.; Singh, S.; Grewal, A.S.; Srivastav, A.L.; Kaushal, J. An extensive review on the consequences of chemical pesticides on human health and environment. *J. Clean. Prod.* **2021**, *283*, 124657. [CrossRef]
176. Mishra, S.; Mishra, S.; Patel, S.S.; Singh, S.P.; Kumar, P.; Khan, M.A.; Awasthi, H.; Singh, S. Carbon nanomaterials for the detection of pesticide residues in food: A review. *Environ. Pollut.* **2022**, *310*, 119804. [CrossRef] [PubMed]
177. Wang, D.; Wang, Y.; Singh, V.P.; Zhu, J.; Jiang, L.; Zeng, D.; Liu, D.; Zeng, X.; Wu, J.; Wang, L.; et al. Ecological and health risk assessment of PAHs, OCPs, and PCBs in Taihu Lake basin. *Ecol. Indic.* **2018**, *92*, 171–180. [CrossRef]
178. Bala, R.; Kumar, M.; Bansal, K.; Sharma, R.K.; Wangoo, N. Ultrasensitive aptamer biosensor for malathion detection based on cationic polymer and gold nanoparticles. *Biosens. Bioelectron.* **2016**, *85*, 445–449. [CrossRef]
179. Ma, T.; Zhou, J.; Wei, D.; Peng, H.; Liu, X.; Guo, W.; Zhang, C.; Liu, X.; Li, S.; Deng, Y. Ultrasensitive Electrochemical Aptasensing of Malathion Based on Hydroxylated Black Phosphorus/Poly-L-Lysine Composite. *Biosensors* **2023**, *13*, 735. [CrossRef]
180. Wang, G.; Liu, J.; Dong, H.; Geng, L.; Sun, J.; Liu, J.; Dong, J.; Guo, Y.; Sun, X. A dual-mode biosensor featuring single-atom Fe nanozyme for multi-pesticide detection in vegetables. *Food Chem.* **2024**, *437*, 137882. [CrossRef]
181. Qiu, J.; He, Z.; Zhao, Z.; Duan, X.; Wang, S.; Shen, J.; Wang, Z.; Chen, H. Advances in electrochemical aptasensors: Aptamer selection, construction and application in food safety. *TrAC Trends Anal. Chem.* **2025**, *191*, 118332. [CrossRef]
182. Shoaib, M.; Li, H.; Zareef, M.; Khan, I.M.; Iqbal, M.W.; Niazi, S.; Raza, H.; Yan, Y.; Chen, Q. Recent Advances in Food Safety Detection: Split Aptamer-Based Biosensors Development and Potential Applications. *J. Agric. Food Chem.* **2025**, *73*, 4397–4424. [CrossRef] [PubMed]
183. Wu, X.; Yuan, Z.; Gao, S.; Zhang, X.; El-Mesery, H.S.; Lu, W.; Dai, X.; Xu, R. Electrochemical Biosensors Driving Model Transformation for Food Testing. *Foods* **2025**, *14*, 2669. [CrossRef] [PubMed]
184. Bolling, B.W.; Chen, Y.Y.; Kamil, A.G.; Oliver Chen, C.Y. Assay Dilution Factors Confound Measures of Total Antioxidant Capacity in Polyphenol-Rich Juices. *J. Food Sci.* **2012**, *77*, H69–H75. [CrossRef]
185. Zhang, H.; Liu, X.; Chen, T.; Ji, Y.; Shi, K.; Wang, L.; Zheng, X.; Kong, J. Melatonin in Apples and Juice: Inhibition of Browning and Microorganism Growth in Apple Juice. *Molecules* **2018**, *23*, 521. [CrossRef]
186. Chen, J.; Park, B. Effect of immunomagnetic bead size on recovery of foodborne pathogenic bacteria. *Int. J. Food Microbiol.* **2018**, *267*, 1–8. [CrossRef]
187. Nikam, P.S.; Palachandra, S.; Kingston, J.J. In vitro selection and characterization of ssDNA aptamers by cross-over SELEX and its application for detection of *S. Typhimurium*. *Anal. Biochem.* **2022**, *656*, 114884. [CrossRef]
188. Ye, H.; Yang, Z.; Khan, I.M.; Niazi, S.; Guo, Y.; Wang, Z.; Yang, H. Split aptamer acquisition mechanisms and current application in antibiotics detection: A short review. *Crit. Rev. Food Sci. Nutr.* **2022**, *63*, 9098–9110. [CrossRef]
189. Abdelbasset, W.K.; Savina, S.V.; Mavaluru, D.; Shichiyakh, R.A.; Bokov, D.O.; Mustafa, Y.F. Smartphone based aptasensors as intelligent biodevice for food contamination detection in food and soil samples: Recent advances. *Talanta* **2023**, *252*, 123769. [CrossRef]
190. Zein, M.I.H.L.; Hardianto, A.; Irkham, I.; Zakiyyah, S.N.; Devi, M.J.; Manan, N.S.A.; Ibrahim, A.U.; Hartati, Y.W. Recent development of electrochemical and optical aptasensors for detection of antibiotics in food monitoring applications. *J. Food Compos. Anal.* **2023**, *124*, 105644. [CrossRef]
191. Gavrilaș, S.; Ursachi, C.Ș.; Perța-Crișan, S.; Munteanu, F.-D. Recent Trends in Biosensors for Environmental Quality Monitoring. *Sensors* **2022**, *22*, 1513. [CrossRef]
192. Hernandez-Vargas, G.; Sosa-Hernández, J.; Saldarriaga-Hernandez, S.; Villalba-Rodríguez, A.; Parra-Saldivar, R.; Iqbal, H. Electrochemical Biosensors: A Solution to Pollution Detection with Reference to Environmental Contaminants. *Biosensors* **2018**, *8*, 29. [CrossRef]
193. Shao, Y.; Yan, T.; Wang, K.; Huang, S.; Yuan, W.; Qin, F.G.F. Soil heavy metal lead pollution and its stabilization remediation technology. *Energy Rep.* **2020**, *6*, 122–127. [CrossRef]
194. Ding, J.; Zhang, D.; Liu, Y.; Yu, M.; Zhan, X.; Zhang, D.; Zhou, P. An electrochemical aptasensor for detection of lead ions using a screen-printed carbon electrode modified with Au/polypyrrole composites and toluidine blue. *Anal. Methods* **2019**, *11*, 4274–4279. [CrossRef]
195. Gao, F.; Zhan, F.; Li, S.; Antwi-Mensah, P.; Niu, L.; Wang, Q. Dual signal-based electrochemical aptasensor for simultaneous detection of Lead(II) and Mercury(II) in environmental water samples. *Biosens. Bioelectron.* **2022**, *209*, 114280. [CrossRef] [PubMed]
196. Inadera, H. Neurological Effects of Bisphenol A and its Analogues. *Int. J. Med. Sci.* **2015**, *12*, 926–936. [CrossRef]
197. Song, Y.; Xu, M.; Li, Z.; He, L.; Hu, M.; He, L.; Zhang, Z.; Du, M. Ultrasensitive detection of bisphenol A under diverse environments with an electrochemical aptasensor based on multicomponent AgMo heteronanostructure. *Sens. Actuators B Chem.* **2020**, *321*, 128527. [CrossRef]
198. Chen, G.; den Braver, M.W.; van Gestel, C.A.M.; van Straalen, N.M.; Roelofs, D. Ecotoxicogenomic assessment of diclofenac toxicity in soil. *Environ. Pollut.* **2015**, *199*, 253–260. [CrossRef] [PubMed]
199. Zou, Y.; Griveau, S.; Ringuedé, A.; Bedioui, F.; Richard, C.; Slim, C. Functionalized Multi-Walled Carbon Nanotube–Based Aptasensors for Diclofenac Detection. *Front. Chem.* **2022**, *9*, 812909. [CrossRef]

200. Wei, N.; Hu, C.; Dittmann, E.; Song, L.; Gan, N. The biological functions of microcystins. *Water Res.* **2024**, *262*, 122119. [CrossRef]
201. Wang, Y.; Li, Y.; Liu, C.; Dong, N.; Liu, D.; You, T. Laser induced graphene electrochemical aptasensor based on tetrahedral DNA for ultrasensitive on-site detection of microcystin-LR. *Biosens. Bioelectron.* **2023**, *239*, 115610. [CrossRef] [PubMed]
202. Noureen, B.; Ullah, N.; Tian, Y.; Du, L.; Chen, W.; Wu, C.; Wang, P. An electrochemical PAH-modified aptasensor for the label-free and highly-sensitive detection of saxitoxin. *Talanta* **2022**, *240*, 123185. [CrossRef] [PubMed]
203. Karazan, Z.M.; Roushani, M.; Hoseini, S.J.; Nasibipour, M. Designing an electrochemical aptasensor based on a microstructure porous-covalent organic polymer for the determination of 2,4,6-trinitrotoluen in water and soil samples. *Microchem. J.* **2024**, *204*, 110975. [CrossRef]
204. Sun, J.; Ji, L.; Li, Y.; Cao, X.; Shao, X.; Xia, J.; Wang, Z. Electrochemical aptasensors based on porous carbon derived from graphene oxide/ZIF-8 composites for the detection of *Erwinia cypripedii*. *Talanta* **2024**, *276*, 126250. [CrossRef]
205. Jarczewska, M.; Sokal, M.; Olszewski, M.; Malinowska, E. Studies on the Aptasensor Miniaturization for Electrochemical Detection of Lead Ions. *Biosensors* **2024**, *14*, 110. [CrossRef]
206. Aydın, E.B.; Aydın, M.; Sezgintürk, M.K. Electrochemical bioplatform for the determination of the most common and carcinogenic dibutyl phthalate migrated from daily-use plastic products. *Microchim. Acta* **2025**, *192*, 548. [CrossRef]
207. Venegas, C.J.; Marin, D.; Miralles-Cuevas, S.; Tamayo, F.; Rodríguez, L.; Sierra-Rosales, P. Electrochemical aptasensor based on carbonized eggshell membranes for carbendazim monitoring in aquatic systems. *Microchem. J.* **2025**, *215*, 114363. [CrossRef]
208. Liu, L.; Yu, H.; Zhao, Q. The Characterization of Binding between Aptamer and Bisphenol A and Developing Electrochemical Aptasensors for Bisphenol A with Rationally Engineered Aptamers. *Biosensors* **2022**, *12*, 913. [CrossRef]
209. Al Borhani, W.; Rhouati, A.; Cialla-May, D.; Popp, J.; Zourob, M. Multiplex electrochemical aptasensor for the simultaneous detection of linomycin and neomycin antibiotics. *Talanta* **2025**, *282*, 126922. [CrossRef]
210. Wang, G.; Sun, J.; Li, B.; Guan, F.; Huang, J.; Dong, H.; Zhang, J.; Han, J.; Shen, Z.; Xu, D.; et al. Multiplex strategy electrochemical platform based on self-assembly dual-site DNA tetrahedral scaffold for one-step detection of diazinon and profenofos. *Sci. Total Environ.* **2023**, *868*, 161692. [CrossRef]
211. Shi, X.; Sun, J.; Yao, Y.; Liu, H.; Huang, J.; Guo, Y.; Sun, X. Novel electrochemical aptasensor with dual signal amplification strategy for detection of acetamiprid. *Sci. Total Environ.* **2020**, *705*, 135905. [CrossRef]
212. Qin, N.; Liu, J.; Li, F.; Liu, J. Recent Advances in Aptasensors for Rapid Pesticide Residues Detection. *Crit. Rev. Anal. Chem.* **2023**, *54*, 3592–3613. [CrossRef]
213. Phopin, K.; Tantimongcolwat, T. Pesticide Aptasensors—State of the Art and Perspectives. *Sensors* **2020**, *20*, 6809. [CrossRef]
214. Nguyen, V.-T.; Kwon, Y.S.; Gu, M.B. Aptamer-based environmental biosensors for small molecule contaminants. *Curr. Opin. Biotechnol.* **2017**, *45*, 15–23. [CrossRef]
215. McConnell, E.M.; Nguyen, J.; Li, Y. Aptamer-Based Biosensors for Environmental Monitoring. *Front. Chem.* **2020**, *8*, 434. [CrossRef]
216. Lupoi, T.; Leroux, Y.R.; Feier, B.; Cristea, C.; Geneste, F. Electrochemical and photoelectrochemical aptasensors for the detection of environmental pharmaceutical pollutants. *Electrochim. Acta* **2025**, *530*, 146396. [CrossRef]

Disclaimer/Publisher's Note: The statements, opinions and data contained in all publications are solely those of the individual author(s) and contributor(s) and not of MDPI and/or the editor(s). MDPI and/or the editor(s) disclaim responsibility for any injury to people or property resulting from any ideas, methods, instructions or products referred to in the content.